Host-Guest Complexes

How to cite:
International Edition: doi.org/10.1002/anie.202214705
German Edition: doi.org/10.1002/ange.202214705

Micromolar Affinity and Higher: Synthetic Host–Guest Complexes with High Stabilities

*Sayan Sarkar, Pablo Ballester, Mark Spektor, and Evgeny A. Kataev**

Angewandte International Edition Chemie

Abstract: The design of high-affinity synthetic host–guest complexes is of paramount importance because they are key elements in constructing unprecedented supramolecular assemblies, functional materials, molecular probes, artificial signal transduction events, and interfaces with the biological world. The present review article collects recent achievements in the design of 1:1 host–guest complexes with outstanding stabilities, i.e., exceeding $10^6\ M^{-1}$. The relationships between the measured thermodynamic constants and the structural parameters of the interacting species are analyzed. The design features of high-affinity hosts are discussed in light of their binding properties. Different solvents and different types of noncovalent interactions are considered for the stabilization of the complexes. Finally, some hints are provided for the design of future synthetic receptors displaying high affinity and selectivity.

1. Introduction

Nature has designed numerous compounds and molecular assemblies having a great variety of properties and functions. One of the most exciting features of natural systems is the high selectivity exhibited in molecular recognition processes. This was described in 1894 by Emil Fischer using a key and lock analogy.[1] It is indeed fascinating how Nature's designs achieve high specificity and binding affinity. Proteins are selective in their binding of not only small molecule but also of macromolecules such as proteins and nucleic acids. This high selectivity is crucial for realizing molecular devices that enable chemical communication, molecular motion, drug delivery, and biological activity. Studies on understanding the selectivity and affinity of host–guest systems are valuable for predicting and understanding protein–ligand interactions that can be used to guide drug design. Thus, the creation of synthetic analogs of natural hosts may yield new analytical sensors, supramolecular catalysts, transporters, and other smart molecular systems. Critical for such artificial systems are high affinity and adequate selectivity against the binding of possible competing molecules in solution. In order to interact with natural systems at the same level as antibodies do, the synthetic hosts require affinity values in the range of 10^6–$10^{10}\ M^{-1}$, which must be maintained in the presence of all constituents of living cells.

Since the beginning of biomimetic chemistry, scientists have tried to model the function of proteins and enzymes related to high-affinity binding.[2] For instance, the biotin–(strept)avidin complex has been an important inspiration for many supramolecular chemists. The complex featuring a K_a of $\approx 10^{13}\ M^{-1}$ represents one of the most thermodynamically stable complexes known to date.[3] The unusually high association constant arises from multivalent hydrogen bonding interactions acting cooperatively. The resulting stabilization overrides the sum of the free energies of the individual interactions.[4] A strong affinity is also observed in the binding of *m*-(*N*,*N*,*N*-trimethylammonio)trifluoroacetophone, which is known to inhibit acetylcholinesterases. The apparent association constant reaches a value of $K_a = 1.2 \times 10^{10}\ M^{-1}$ with dissociation rate constants on the order of $10^{-5}\ s^{-1}$.[5] The natural cyclic depsipeptide valinomycin recognizes the potassium cation with high K^+/Na^+ selectivity and facilitates the potassium transport across the biological membrane. Binding investigations showed that the complex affinity ranged from 10 to $10^6\ M^{-1}$ depending on the solvent mixture used for the measurements.[6] Such a wide range of binding affinities might be a key parameter for good membrane permeability and transport. Choline binding protein ChoX has a unique aromatic cavity that inspired many researchers to design synthetic receptors featuring hydrophobic cavities which are able to isolate the guest from interacting with bulk water molecules. ChoX is responsible for the strong binding with choline ($K_a = 3.7 \times 10^6\ M^-$) and acetylcholine ($K_a = 6.9 \times 10^3\ M^{-1}$).[7] Cation–π interactions play a decisive role in stabilizing the complex, which displays the alkylammonium guests included deep in the protein's cavity.[8]

Houk and co-workers demonstrated in their review article that on average synthetic hosts underperform the binding properties of natural systems by six orders of magnitude. The average binding affinities for biological recognition processes, such as the complexation of transition states and the binding of antigens with antibodies, are $10^{8\pm2}\ M^{-1}$. This is a challenging magnitude for the researchers who design synthetic host–guest complexes trying to mimic natural proteins. In short, approaching the "protein-like" affinities using synthetic receptors is highly demanding. Nevertheless, the number of synthetic hosts that bind guest molecules with affinity values larger than $K_a = 10^6\ M^{-1}$ has dramatically increased in the recent decade. Notably, these hosts will be able to bind their target molecules, to a significant extent, in concentrations as low as 1 μM. However, there are still many open questions to answer and challenges to undertake, such as: How should we design high-affinity synthetic hosts? What kind of noncovalent interactions should be involved in the design? How can we enhance the binding affinity of already known systems? Can

[*] S. Sarkar, M. Spektor, E. A. Kataev
Department of Chemistry and Pharmacy
Friedrich-Alexander Universität Erlangen-Nürnberg
Nikolas-Fiebiger-Str. 10, 91058 Erlangen (Germany)
E-mail: evgeny.kataev@fau.de

P. Ballester
ICREA
Passeig Lluís Companys 23, 08010 Barcelona (Spain)

P. Ballester
Institute of Chemical Research of Catalonia (ICIQ)
The Barcelona Institute of Science and Technology (BIST)
Av. Països Catalans, 16, 43007 Tarragona (Spain)

we create hosts that make good use of cooperative noncovalent interactions? How can we achieve strong binding in the host–guest system and make it solvent-independent?

How much is $10^6\ M^{-1}$ affinity? In terms of free energy, this is less than $-35\ kJ\,mol^{-1}$ or $-8.3\ kcal\,mol^{-1}$ at 25 °C. The free energy provided by one hydrogen bond in an amide–amide interaction (CONH···O=CNH) in an organic solvent such as chloroform is approximately 5–8 $kJ\,mol^{-1}$. Thus, to reach micromolar affinity, we would need the establishment of at least four or five hydrogen bonds (not considering secondary interactions) between the host and guest. This is indeed the case for dimers stabilized by an array of hydrogen bonds, which reach dimerization constant values on the order of $10^9\ M^{-1}$.[9] Interestingly, for many hydrogen-bonded supramolecular systems, the additivity rule does not work. In Watson–Crick base pairs, the relative thermodynamic stability is not directly related to the number of hydrogen bonds. For example, the GC pair (guanine–cytosine) contains one more hydrogen bond than the AT pair (adenine–thymine). Thus, one would expect increased free energy of ca. 50 %. However, experimentally, the binding energy for the GC pair increases 190 % with respect to that of the AT counterpart. Theoretical calculations suggested that partial charge patterns (secondary interactions) may contribute to the overall free binding energy.[10]

To assess the cooperativity of separate binding sites in a host–guest complex featuring N binding sites, the calculation of effective molarity (EM) can be very helpful.[11] Essential for these systems is the consideration that only the first interaction is intermolecular, while the rest are intramolecular. EM is determined as the ratio K_a/K_{ref}^{N}, where K_a is the apparent association constant determined for the host–guest complex, and K_{ref} is the affinity of a single binding site. Thus, the EM K_{ref} value serves as an indicator of cooperativity. When it is larger than one, a preferable assembly of a closed 1:1 complex (chelate) involving an intramolecular interaction should occur.

Other structural parameters may also affect the overall binding energy of the complex. These include steric factors, the occurrence of tautomeric structures, the presence of repulsive interactions, and finally, the ground state conformations of the free partners in the solution. In water, coulombic or charge–charge interactions often contribute to the energy of binding with a similar contribution of about $5\ kJ\,mol^{-1}$, and in many cases, they are simply additive. This fact explains the high binding constants of many polyammonium synthetic receptors for negatively charged guests.[12] In many instances, the more critical factor affecting the magnitude of the free binding energy of the complex is the solvent in which the binding takes place. In many of the cases that will be discussed below, solvation/desolvation processes are determinants of the magnitude of the binding affinity. These processes can be independent of the host–guest complementarity (size, shape, and functionality) and the nature of the noncovalent interactions established between them.

The goal of this review article is to overview a series of examples of synthetic host–guest systems featuring strong binding affinities. The selected examples have binding constants exceeding a value of $10^6\ M^{-1}$ and produce a simple 1:1 stoichiometric complex (micromolar affinity). We analyze the origins of these high-affinity values on the basis of

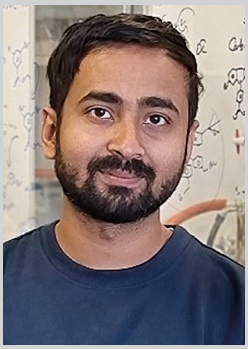

Sayan Sarkar received his M.Sc. in Chemistry at Presidency University, Kolkata (India). He obtained his Ph.D. with Prof. Pradyut Ghosh from Indian Association for the Cultivation of Science (IACS Kolkata). Currently, he is working as a postdoctoral researcher with Prof. Evgeny Kataev at Friedrich-Alexander University Erlangen-Nürnberg (Germany). His current research focuses on synthesizing macrocyclic aromatic hydrocarbons and their application in host–guest chemistry.

Pablo Ballester studied Chemistry at the University of the Balearic Islands (UIB), where he also completed his Ph.D. in 1986 (Prof. Ramón Mestres). He worked as a postdoctoral fellow with Prof. Julius Rebek, Jr. at the University of Pittsburgh and MIT (USA) for three years and one year at the UIB (Prof. José M. Saá). In 1990, he joined UIB as an Assistant and Associate Professor. In 2004, he was awarded an ICREA Research Professorship and moved to the Institute of Chemical Research of Catalonia (ICIQ, Spain). His research interests are in the areas of molecular self-assembly, molecular recognition, and supramolecular catalysis.

Mark Spektor studied Chemistry at the Friedrich-Alexander University, Erlangen-Nürnberg (Germany). He joined the Kataev group in the fall of 2022 as a Ph.D. student. His work focuses on macrocyclic aromatic hydrocarbons and their application in host–guest chemistry.

Evgeny A. Kataev studied Chemistry at the M.V. Lomonosov Moscow State University (2003). He obtained his Ph.D. in 2006 from the joint program of MSU (Prof. Yuri A. Ustynyuk) and the University of Texas at Austin (Prof. Jonathan L. Sessler). He was a postdoctoral fellow at EPFL Lausanne (Prof. Kay Severin) and the University of Regensburg (Prof. Burkhard König). In 2011 he joined TU Chemnitz as a junior professor. In 2019 he was an interim professor at FAU Erlangen-Nürnberg, and since April 2020 he has continued at FAU as a Heisenberg Fellow. His research interests are in the areas of organic synthesis, supramolecular recognition, and sensing in water.

structural and energetics considerations. Practically, the level of binding affinity/stability of the complexes is strongly dependent on solvent, concentration, determination method, and pH of the solution. However, in this review, we consider synthetic receptors able to form 1:1 complexes with binding stabilities larger than $10^6\ M^{-1}$ independent of the conditions used in the thermodynamic characterization. We believe that the formation of a 1:1 complex with high affinity ($K_a > 10^6\ M^{-1}$) independent of the conditions used (solvent, pH etc.) can by itself be considered as a great achievement. We exclude from our review strong binders such as coordination metal complexes and cucurbituril inclusion complexes, which have been thoroughly discussed in recent review articles.[13] These host–guest systems were used in sensing displacement assays with dyes,[14] in the construction of functional and stimuli-responsive materials,[15] and in medicinal chemistry.[16]

This review is divided into three major sections dealing with the recognition of differently charged guest molecules: neutral, positively, and negatively charged. We comment on the molecular design approaches used to achieve strong binding. We detail the thermodynamic signature of the binding processes in the cases where the data are available. The last section and the conclusions are devoted to underlining the origins of strong binding in synthetic host–guest systems. Using the available thermodynamic data of the discussed examples, we build several correlations, which we expect will be helpful in providing some hints for the successful design of the next generation of synthetic receptors.

2. Binding of Neutral Guests

Fullerenes remain appealing targets for the construction of supramolecular host–guest complexes.[17] Using such supramolecular systems can considerably broaden and strengthen the applications of fullerenes in semiconductor technology, solar cells, batteries, and biomedical areas.[18,19] Moreover, unprecedented hierarchical hybrid nanostructure with new properties can be constructed and explored using the host–guest chemistry of fullerene derivatives.[20]

A series of carefully designed macrocycles based on porphyrin units were reported by the Anderson group. For example, macrocycle **1** exhibited high binding affinities for fullerenes owing to the good fit of its cavity with the size and shape of the fullerenes. The determined association constants for the fullerenes in the toluene solution were remarkable: 2.0×10^6 and $2.0\times10^8\ M^{-1}$ for C_{60} and C_{70}, respectively. This result indicated that **1** possessed close to 100-fold selectivity in the binding of C_{70} over C_{60} (Figure 1).[21] Strong binding to La@C_{82}, a paramagnetic endohedral metallofullerene, was successfully achieved by Aida and co-workers.[22] They constructed covalent cage **3**, which consists of two copper(II) porphyrin complexes connected by four spacers. Receptor **3** was prepared via a metathesis reaction from the precursor complex **2**⊃La@C_{82}, likely serving as a template. The number of spacers between the porphyrin rings appeared to play an important role in binding. After the formation of cage **3**, the affinity for the fullerene derivative increased in one order of magnitude: from 1.5×10^6 to $1.5\times10^7\ M^{-1}$ (toluene).

Ribas and co-workers developed a palladium self-assembled cage **6**. Cage **6** was constructed using four copies of the dipalladium polyammonium-based macrocycle **4** and two copies of the tetraamine porphyrin **5**.[23] The cage was assembled in a toluene/acetonitrile 1:1 solution with a remarkably high yield (Figure 1). Cage **6** has the unique ability to adapt its cavity geometry and volume to that of fullerene derivatives of different sizes (from C_{60} to C_{84}). The cage was found to possess a sponge-like behavior, which was utilized for removal of C_{60} from a mixture of fullerenes. High binding affinities of the complexes were determined using UV/Vis titrations. For instance, the association constant of **6** with C_{60} in a 1:1 acetonitrile/toluene solvent mixture was calculated as $K_a = 2.8\times10^7\ M^{-1}$ (UV/Vis) and $K_a = 2.9\times10^7\ M^{-1}$ (fluorescence). The complexation of **6** with C_{70} was even stronger: $K_a = 4.0\times10^8\ M^{-1}$ (fluorescence). In subsequent work, the binding of cage **6** with C_{60} was studied in a 1:1 CH_2Cl_2/toluene solvent mixture resulting in an association constant (K_a) of $3.6\times10^7\ M^{-1}$. In this solvent system, it was possible to mask fullerene to enable its selective equatorial functionalization via Bingel–Hirsch cyclopropanation. The authors succeeded in converting this reaction into a catalytic process by using biphasic conditions, yielding the quantitative regioselective functionalization of C_{60}.[24]

Aida reported on iridium and rhodium porphyrins covalently connected to form the macrocyclic scaffolds **7a**,**b**. These macrocycles were able to form thermodynamically highly stable complexes with C_{60} and C_{70}.[25] The binding constant determined for the iridium complex was larger than $10^9\ M^{-1}$ in benzene. Thus, the more polar *ortho*-dichlorobenzene (o-DCB) was used as a solvent to decrease the binding affinity owing to the improved solvation of the binding partners. However, the determined value of the binding constant $K_a = 1.3\times10^8\ M^{-1}$ was still very large. The binding with the iridium macrocycle represented a particular case. Iridium coordinates through η^2 hapticity to a C–C junction in fullerene. NMR investigations showed that the coordination bond was dynamic. Cooling the solution yielded a broader ^{13}C signal for fullerene, which also supported the rotary motion of the guest.

An interesting case of fullerene recognition by curved porphyrins was described by the Delius group. The authors successfully prepared two nanohoops [2]CPT (**8**) and [2]CPTN (**9**) containing two nickel(II) porphyrin complexes.[26] The binding affinities of [2]CPT, **8**, for C_{60} and C_{70} were determined in toluene solution as $3.0\times10^8\ M^{-1}$ and $2.0\times10^7\ M^{-1}$, respectively. The increase in the contact area of the complexes contributed significantly to the binding compared to the parent [10]CPP macrocyclic receptor,[27] which showed a 100-fold weaker affinity for C_{60}. The introduction of a naphthalene unit in the macrocyclic scaffold of receptor **9** did not change the binding affinity for C_{60} ($3.0\times10^8\ M^{-1}$). This unexpected finding was attributed to the high energy of deformation of the host upon complex formation. This hypothesis was also supported by the larger

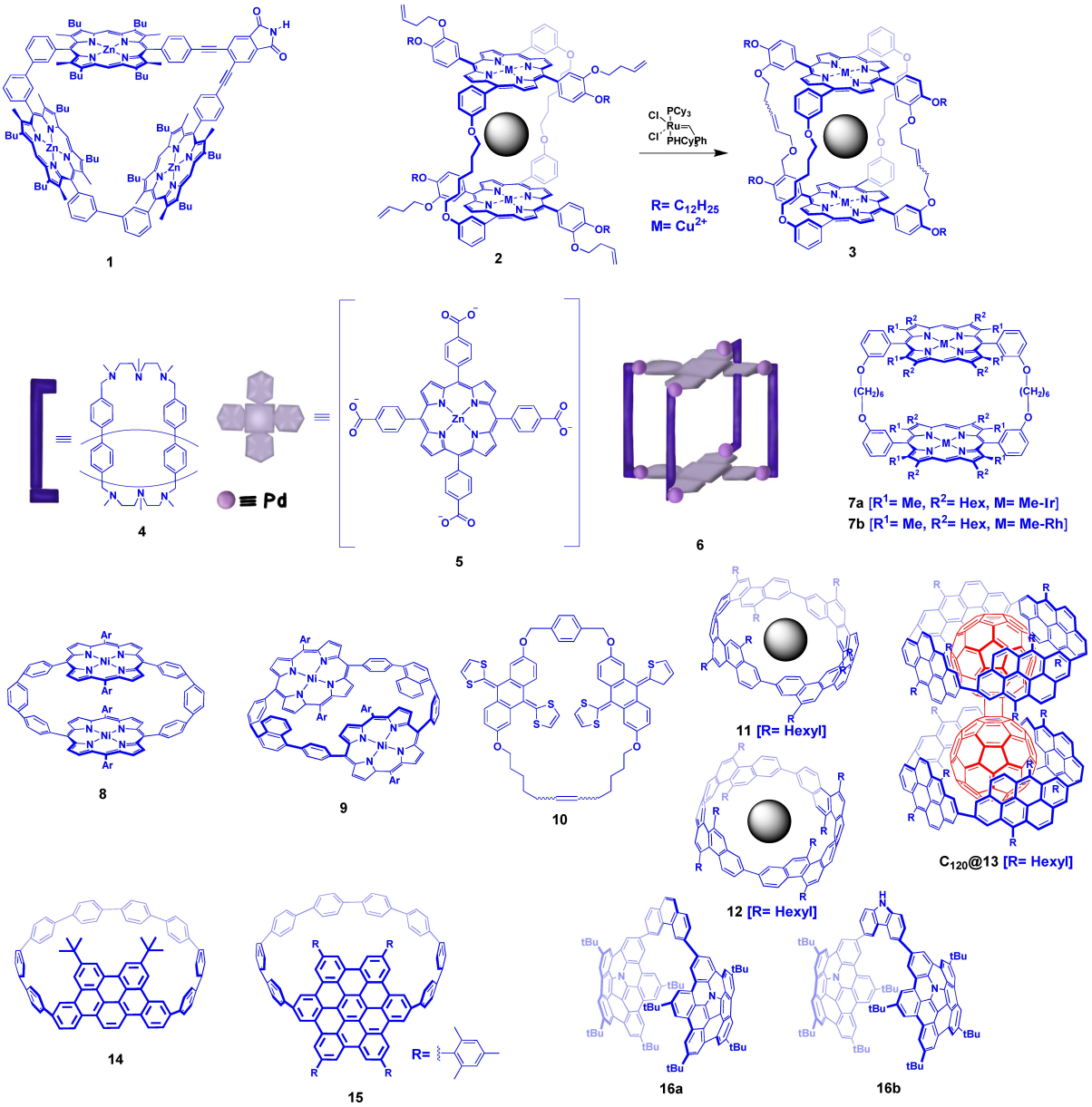

Figure 1. Structures of the synthetic receptors used for the recognition of fullerenes.

binding affinity displayed by [2]CTPN (**9**) upon binding C_{70}. Probably, the increase in the contact surface area of the complex owing to the larger size of C_{70} compensated for the deformation energy of the bound host.

Extended tetrathiafulvalenes (exTTF, 2-[9-(1,3-dithiol-2-ylidene)anthracen-10(9*H*)-ylidene]-1,3-dithiols) are electron-rich moieties that form thermodynamically stable complexes with C_{60} ($K_a = 3.9 \times 10^3\ M^{-1}$in chlorobenzene). The Martin group constructed tweezer-like receptors by covalently connecting two exTTF units through two differently sized spacers yielding macrocycle **10**. This simple design allowed the authors to achieve C_{60} binding at micromolar concentrations in chlorobenzene solution ($K_a = 3.0 \times 10^6\ M^{-1}$).[28] Extraordinarily high binding affinities for fullerenes were reported by the Isobe group, who explored variations in the contact area of the receptors with a series of fullerene derivatives. For instance, the calculated binding constant values for **11** (in *ortho*-dichlorobenzene solvent) with $Li^+@C_{60}{\cdot}PF_6^-$ ($K_a = 1.2 \times 10^9\ M^{-1}$) and $H_2O@C_{60}$ ($K_a = 1.6 \times 10^9\ M^{-1}$) were slightly lower than those for C_{60} ($K_a = 3.9 \times 10^9\ M^{-1}$) and C_{70} ($K_a = 5.0 \times 10^9\ M^{-1}$). The authors suggested that the small difference in diameter of the series of fullerene derivatives could be essential in determining the magnitude of the binding affinity.[29] Four other isomeric receptors, including **12** were later studied in detail in order to establish their binding abilities for C_{60}.[30] The isomeric receptors have diameters of 1.24–1.37 nm, which perfectly fit the sizes of the investigated guests. Binding studies in different solvents revealed the existence of a very strong affinity of **11** for C_{60} ($K_a = 2.0 \times 10^{12}\ M^{-1}$) in benzene solution.

The lower the solubility of C_{60} was in a particular solvent, the larger was the determined binding constant of the complex owing to its superior solubility. The solubility of C_{60} in the solvent series decreased in the following order *o*-DCB (*o*-dichlorobenzene) < PhCl < $CHCl_3 \approx CH_2Cl_2$ < toluene < benzene. Remarkably, although the formation of the complex is only driven by solvophobic effects and dispersion interactions, a 1:1 complex featuring a high stability constant is produced, whose magnitude is close to that of the biotin–streptavidin counterpart. Notably, the binding affinity of **12** for C_{60} was more than four orders of magnitude smaller than that of other macrocycles. Nevertheless, **12** bound C_{60} ($K_a = 2.0 \times 10^4\ M^{-1}$) still more strongly than [10]CPP ($K_a = 6.3 \times 10^3\ M^{-1}$ in *o*-DCB). The authors suggested that the fluctuation of the aromatic walls in the belt might play a significant role for binding. This conclusion is similar to that made by the Delius group regarding the binding affinity values of receptors **8** and **9**: the receptor's preorganization was key in determining the magnitude of the binding affinity.

The binding of the belt-shaped cylindrical molecule **13**, having a persistent geometry, was further investigated with the larger guest C_{120}. This guest can bind two macrocycles in a stepwise process. It was found that **13** bound C_{120} through a non-cooperative stepwise binding process with $K_{a1} = 6.9 \times 10^8\ M^{-1}$ and $K_{a2} = 3.2 \times 10^3\ M^{-1}$. Receptor **11** showed slightly stronger binding affinities in the binding of C_{120} in *o*-DCB solution: $K_{a1} = 1.4 \times 10^9\ M^{-1}$ and $K_{a2} = 4.5 \times 10^5\ M^{-1}$.[31] The more significant difference was detected in the second binding event leading to the formation of a 1:2 complex. However, this observation can be explained by the fact that the two receptors in the $C_{120}\subset(\mathbf{13})_2$ complex experience steric repulsion since they are larger in size than **11**.

An alternative approach to form a belt-like host for C_{60} was proposed by Yang and Du.[32] The authors synthesized two macrocycles, **14** and **15**, containing hexabenzocoronene and pentaphene subunits, respectively, and resembling a crown. According to the binding investigations performed in CH_2Cl_2 solution, the stability constants for the complexes C_{60}@**14** and C_{60}@**15** were calculated to be $3.3 \times 10^6\ M^{-1}$ and $2.3 \times 10^7\ M^{-1}$, respectively. The increased stability for the latter complex was explained by the extended π-conjugation of the receptor's binding units. The complexation of C_{70} with affinity $1.1 \times 10^6\ M^{-1}$ in toluene was recently achieved by a macrocycle consisting of four hexa-*peri*-hexabenzocoronene subunits.[33] As a possible application of such supramolecular systems, the authors demonstrated their ability to generate significant photocurrent upon light irradiation when incorporated in FTO glass substrates of solar cells.

Nitrogen- containing Bucky bowl units are known to bind C_{60} with a relative association constant $K_a = 6.2 \times 10^4\ M^{-1}$ in toluene solution.[34] The idea behind the molecular design of the tweezers **16a**,**b** was to combine two such units with an appropriate linker to achieve high complementarity for fullerene binding. Receptor **16a** (carbazole spacer) was found to bind C_{70} ($K_a = 7.0 \times 10^8\ M^{-1}$) more strongly than C_{60}. ($K_a = 4.4 \times 10^7\ M^{-1}$) in toluene. In contrast, receptor **16b** (phenanthrene spacer) complexed C_{60} more strongly ($K_a = 3.0 \times 10^8\ M^{-1}$) than C_{70}. ($K_a = 6.3 \times 10^7\ M^{-1}$). The difference in the binding constants confirmed the effect of the preorganization of the two tweezer arms in fullerene binding. The carbazole spacer positioned the arms of the tweezers at a distance more suitable for the inclusion of the larger fullerene.

Diederich was one of the first in showing the ability of positively charged and water-soluble macrocycles (cyclophanes) to bind aromatic substrates with high affinity in water.[35] Solid–liquid extraction experiments revealed the high binding affinities of macrocycle **17** for perylene ($K_a = 1.6 \times 10^7\ M^{-1}$), fluoranthene ($K_a = 1.2 \times 10^6\ M^{-1}$), and pyrene ($K_a = 1.1 \times 10^6\ M^{-1}$) (Figure 2). Negatively charged aromatic dyes like anilinonaphthalene-8-sulfonate (ANS) ($K_a = 3.2 \times 10^6\ M^{-1}$) and 3,5-dinitrosalycylic carboxylate (DNS) ($K_a = 1.4 \times 10^5\ M^{-1}$) were also bound with high affinity by positively charged macrocycles. However, the magnitude of the binding constants for the neutral guests exceeded those of their negatively charged counterparts. The obtained results demonstrated that charge–charge interactions were not the most important contributors to the binding of negatively charged hydrophobic molecules in an aqueous solution.

An in-depth investigation of solvent effects on the complexation of pyrene by cryptand **18** was carried out.[36] A linear free energy relationship was observed with the Dimroth–Reichard polarity parameter of the solvent $E_t(30)$. Thus, the binding strength of the pyrene⊂**18** complex was determined by the solvent polarity increasing from $K_a = 9\ M^{-1}$ in CS_2 to $K_a = 6.0 \times 10^6\ M^{-1}$ in water. Water is the best solvent to drive apolar host–guest binding (hydrophobic effect). Water possesses the highest cohesive interactions and the lowest molecular polarizability maximizing solvation/desolvation effects of host, guest, and the complex. Bria et al. found that cyclobis(paraquat-*p*-phenylene) **19** was soluble in water and coordinated with guests **G1** and **G2**, producing 1:1 complexes with [2]pseudorotaxane topology.[37] The additional phenyl ring in the structure of **G2** had a significant effect on the binding affinity. The binding stability of complex **19**·**G1** is only $K_a = 7.3 \times 10^3\ M^{-1}$, while that of the **19**·**G2** complex is about 200-fold larger—$K_a = 1.5 \times 10^6\ M^{-1}$. Apparently, the dramatic increase in binding affinity is caused by the larger contact surface area of complex **19**·**G2**. This observation correlates well with the results obtained for cyclophane **18**, indicating the importance of the release of solvent molecules involved in the solvation of the binding partners to the bulk solution (desolvation) prior to binding.

Receptors **20** and **21** were designed to bind octyl glucosides and native saccharides in an organic solution (dichloroethane).[38] The main polar binding sites of the receptors for the coordination of the sugar hydroxyl groups were phenol, as a hydrogen bond donor, and pyridine, as a hydrogen bond acceptor. Binding studies were monitored using circular dichroism (CD) spectroscopy revealing large binding affinities for e.g., octyl-β-glucose ($K_a = 10^7\ M^{-1}$ for receptor **20**) and octyl-β-galactose ($K_a = 5.3 \times 10^7\ M^{-1}$ for receptor **21**). The fact that most binding constants of the complexes of the sugar derivatives with the tripodal and the cage receptor were larger than $10^6\ M^{-1}$ supported the importance of the receptor's preorganization in achieving

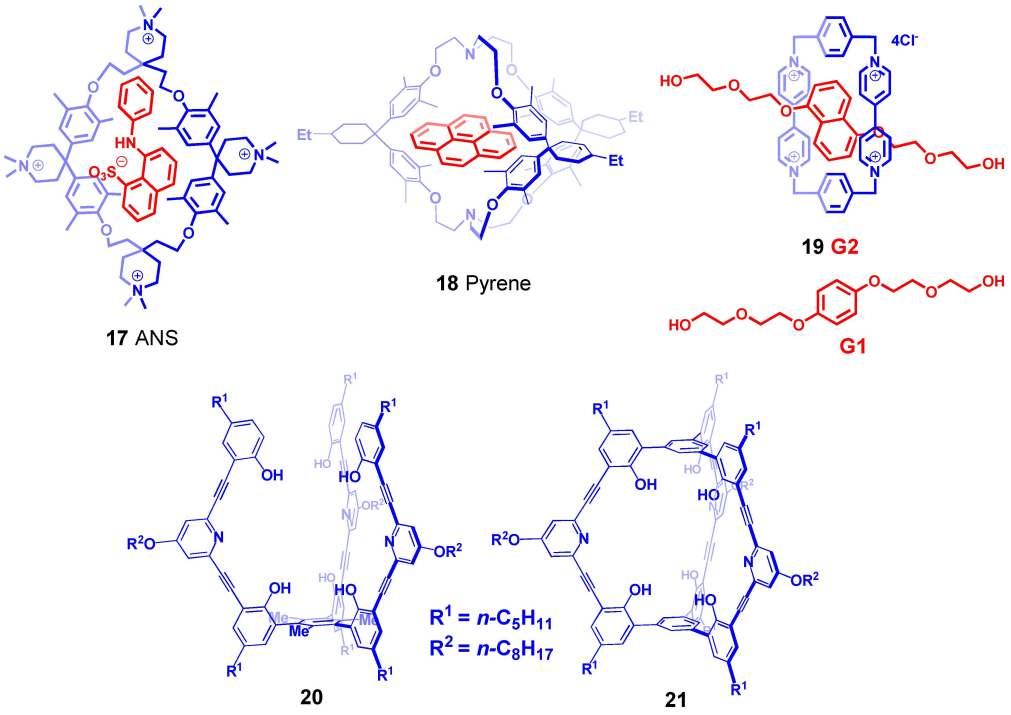

Figure 2. Structures of macrocyclic receptors for neutral guests.

strong binding. The binding selectivity of receptors **20** and **21** was slightly different. Most likely, the similar binding behavior of the two receptors is restricted to the use of nonpolar solvents. We believe that the binding properties of the two receptors would be significantly different in polar solvents owing to the dissimilar exposure of their polar binding sites to bulk solvent molecules.

A completely different approach for the binding of sugar derivatives with synthetic receptors was pursued by the Davis group. The authors combined polar interactions with solvophobic effects in the design of the "temple" receptors. They demonstrated that the used solvent produced a significant difference in binding behavior. In pure chloroform solution, sugar derivatives were bound with binding affinities (K_a) larger than $10^6\,M^{-1}$, e.g., 1:1 complex of receptor **22** with cellobiose (Figure 3).[39] However, the binding affinity of the receptors dropped dramatically to $500\,M^{-1}$ in pure water. Most likely, the strong solvation of the –OH groups of the sugars and the polar functions of the receptors exerted by water molecules are responsible for the significant reduction in affinity. Hamilton receptor **23** is a classic example of high complementarity (size, shape, and functional groups) for barbital. The formed 1:1 complex represents an excellent example of a supramolecular system bearing hydrogen bond acceptors and donors in both binding partners. Similarly to the sugar complexes with the "temple" receptors, the thermodynamic stability of the barbital:**23** complex experienced a significant reduction upon the addition of protic solvents. Protic solvents compete with the host–guest hydrogen bonding interactions by solvating the polar binding sites of the free binding partners. The stability constant of barbital:**23** complex in chloroform was $K_a = 1.4 \times 10^6\,M^{-1}$.[40] The hydrogen-bonding array motif of the complex is often used for the construction of supramolecular assemblies and materials. For instance, we recently reported iron oxide nanoparticles functionalized with derivatives of the Hamilton receptor.[41]

The Smith group studied a series of unprecedented host–guest complexes **24** based on the tetralactam macrocycle receptor bearing two anthracene sidewalls. Remarkably, strong association constants were determined for the 1:1 complexes of **24a** with threaded guests. The macrocycle was able to bind the deep-red fluorescent squaraine dye **G5** in chloroform solution with an affinity constant of $K_a = 10^6\,M^{-1}$.[42] The included dye formed hydrogen bonds with the amide NH groups of the receptor and complementary stacking (π–π) interactions with the anthracene walls. The squaraine dye and the host were also functionalized with water-solubilizing groups (polyethylene glycol and carboxylic acid groups), and formed the highly stable 1:1 complex **24b**·**G5**. This complex displayed thermodynamic stability in the range of $10^9\,M^{-1}$ in water solution. This value represented a 1000-fold increase in binding stability compared to the analogous complexes formed in chloroform and methanol solutions.[43] Notably, the determined rate constants of complexation (k_{on}) were also 1000 times faster in water than in methanol, demonstrating the effect of the former in facilitating the assembly of the complex owing to a faster desolvation/solvation process. Likewise, the kinetic stability of the complexes (k_{off}) was reduced in the protic solvents. The kinetic and thermodynamic properties of the complexes, as well as the strong turn-on fluorescence response produced by the binding of the amidosquaraine dyes were implemented in a fluorescent assay to detect liposome

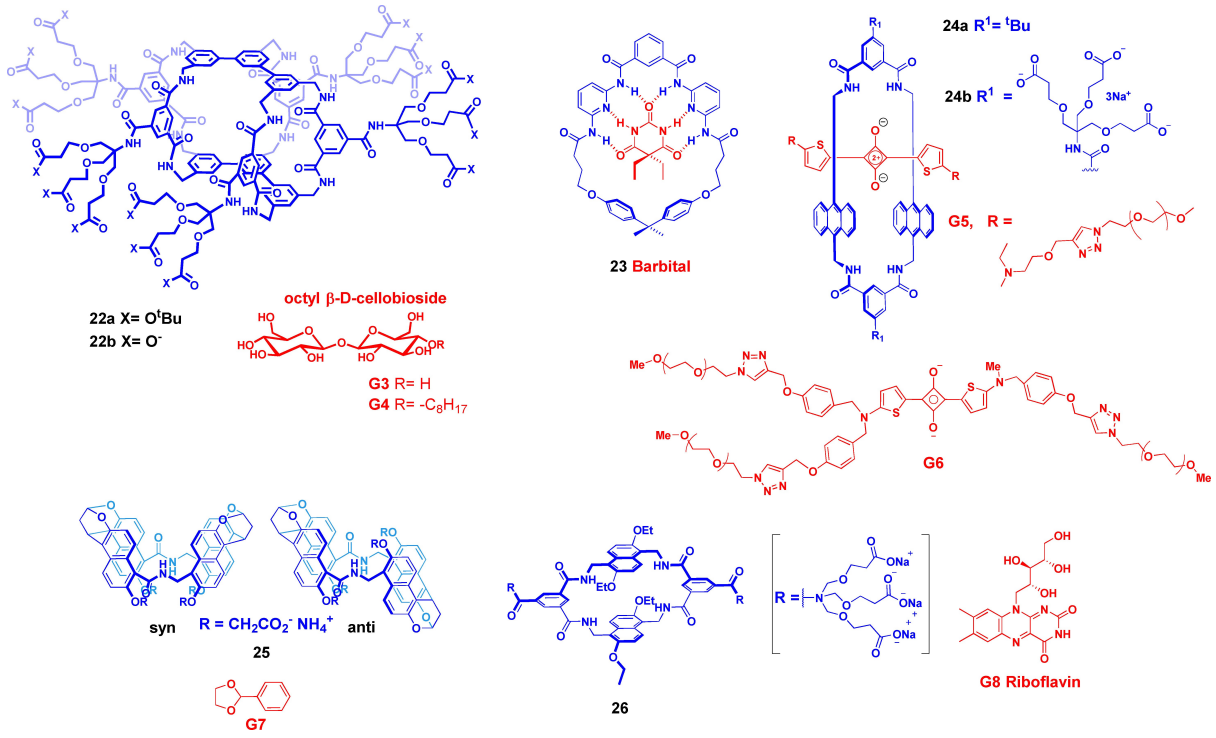

Figure 3. Structures of synthetic receptors for neutral organic compounds.

leakage.[44] Why was it possible to transfer the binding event from chloroform to water winning in binding affinity? The answer to this question lies in the hydrophobic effect being the most important force to drive the binding event. The authors also disclosed an efficient strategy to enhance the host–guest binding up to $5.1\times10^{10}\,M^{-1}$.[45] In **G6** the axles were redesigned with the purpose of introducing additional interactions between the host and guest partners. It was proposed that the additional phenyl rings stack with the 1,3-benzenedicarboxamide or anthracene fragments of the receptor. Kinetic measurements showed that the threading of **G6** also took place very rapidly with $k_{on}=7.9\times10^{7}\,M^{-1}s^{-1}$. In short, a simple strategy of enlarging the surface contact of the binding partners in the complex can provide an increase in binding affinity of approximately 50-fold.

The Jiang group pursued the binding of small hydrophobic and hydrophilic guests in water with high affinity.[46] The key design of host **25** resided on the three-dimensional structure provided by the *endo*-functionalized molecular tube. According to the authors, polar groups should be located inside the deep hydrophobic cavity to favor e.g., hydrogen bonds, by completely avoiding or reducing the hydrogen-bonding competition with bulk water molecules. A total of 44 small molecules were investigated as guests of **25** in a water solution. The guest was bound in the receptor's cavity with binding affinities (K_a) ranging from 8 to $10^6\,M^{-1}$. A principle component analysis of the extensive obtained data showed the existence of a weak correlation between binding strength and hydrophobicity, volume, surface area, or dipole moment of the guests. A combination of host–guest hydrophobic interactions and the release of water molecules from the host cavity (hydrophobic effect), together with the formation of complementary hydrogen bonds, were the decisive factors in determining the complexes' binding affinity. Remarkably, only guest **G7** was bound by **25** with a binding affinity (K_a) larger than $10^6\,M^{-1}$. Most likely, **G7** was the best fit for the cavity of **25** in terms of hydrophobic and polar interactions. Recently, the group discovered that receptor **25** could also bind a range of positively charged dyes with high affinity in water solution.[47]

Cyclodextrins and cucurbiturils are able to bind riboflavin **G8** inside their nonpolar cavities with binding constants that do not exceed $10^4\,M^{-1}$.[48] However, biological transporters reach association strength on the order of $10^9\,M^{-1}$ in water. Tetralactam macrocycle **26**, possessing a polar aromatic interior and an exterior equipped with multiple ionizable groups, was designed by Jiang and coworkers to recognize riboflavin in water by means of the hydrophobic effect, dispersion, and hydrogen bonding interactions. ITC measurements revealed a high-affinity binding ($K_a=1.2\times10^7\,M^{-1}$) for the 1:1 complex, which was dominated by the enthalpy component ($\Delta H=-48.3\,kJ\,mol^{-1}$, $T\Delta S=-7.7\,kJ\,mol^{-1}$). This thermodynamic signature is consistent with a binding process involving the release of so-called "high-energy" water molecules, accompanied by a large enthalpy change. An interesting application of the **G8**⊂**26** complex was to protect riboflavin from degradation caused by UV light irradiation. A similar biomimetic strategy was used by the Jiang group to bind quinones with high binding affinity $K_a>10^9\,M^{-1}$ in an aqueous solution.[49] Receptor **27** was endowed with a

hydrophobic aromatic cavity *endo*-functionalized with two convergent amide bonds (Figure 4). The amide NH groups were responsible for the formation of complementary hydrogen bonding interactions with oxygen atoms of the quinone. Detailed investigations suggested that additional binding stabilization was provided by C–H···π and charge transfer interactions, which were established between the anthracene walls of the receptor and the bound quinone. The binding affinity of receptor **27** for *p*-benzoquinone was determined to be $3.1\times10^4\ M^{-1}$. Binding investigations of receptor **27** with anthraquinone **G9** revealed a larger binding affinity ($K_a=1.5\times10^9\ M^{-1}$) in an aqueous solution.

The incorporation of anthracene units to shape a hydrophobic cavity in metal-mediated supramolecular receptors was efficiently utilized by the Yoshizawa group.[50] The authors explored the host–guest properties of receptor **28** featuring an anisotropic contracted framework with respect to that of previous metallo-capsules reported by the same group. Porphyrin, coronene, and sumanene (**G10**) were investigated as potential guests. The binding constants were difficult to determine accurately owing to their large values. The 1:1 host–guest ratio and the quantitative formation of the sumanene complex were determined by NMR and ESI-TOF MS analyses. In particular, the ^{1}H NMR spectrum of **G10**⊂**28** displayed a complex set of signals in the aromatic region, indicating the desymmetrization of the apparent D_4-symmetric free receptor to a C_4-symmetric 1:1 complex. The bowl-to-bowl inversion of the bound sumanene was discovered to be accelerated through a cavity-induced compression effect.

Coordination cages were shown to be highly efficient for the encapsulation of planar guest molecules. The Stoddart group prepared XCage **29** having an extended aromatic cavity able to bind a perylene-diamide (PDI) dye in water with one of the largest binding affinities so far reported, K_a (PDI⊂**29**) $=7.7\times10^{10}\ M^{-1}$ (Figure 4).[51] The encapsulation of the PDI derivative **G11** had several distinctive features. For example, PDI fluoresces with yellow color and 66 % quantum yield in acetonitrile solution. If water is used as a solvent, the fluorescence of PDI is quenched due to aggregation. However, the addition of receptor **29** led to the deaggregation of the dye and the concomitant formation of the PDI⊂**29** complex having a fluorescence quantum yield of 63 %, a level which is quite close to that of the free dye in acetonitrile solution.

Many cage-like hosts dramatically modify the properties of the included guest molecules, such as absorption and fluorescence spectra, chemical reactivity, and redox potentials. For instance, Fujita explored the interaction of host **30** with tetraazaporphine (**G12**) in water leading to an interesting change in the porphyrin emission.[52] Inside the cavity of **30**, **G12** emitted light with a quantum yield of 0.17. In contrast, the fluorescence of the free guest in water was quenched due to its strong tendency to aggregate. The acidity of the NH groups of the porphyrin **G12** included in the cavity of **30** was higher than in the free state. For this reason, the fluorescence of bound **G12** was switched off by the addition of a base. Another example showing the effect of confined space was reported for porphyrin cage **31**.[53] In water, the host was able to bind the tripeptide Ac-Ala-Ala-Ala-NH_2 (**G13**) in its cavity forcing it to fold in a β-turn conformation despite its short length. The structure of the bound tripeptide was considered to be a minimal 3_{10}-helix. Competitive ^{1}H NMR titrations were used to determine that the binding affinity of cage **31** for the tripeptide was of the order of $K_a=1.0\times10^6\ M^{-1}$.

Ward and co-workers investigated the encapsulation properties of coordination cage $[Co_8L_{12}](BF_4)_{16}$ (**32**) towards a series of cyclic ketones.[54] The affinities of the guests were determined with the help of fluorescence displacement assays using 4-methyl-7-aminocoumarin as an indicator. The strong binding observed in water was mainly driven by the hydrophobic effect, with the highest affinity measured for cycloundecanone **G14** ($K_a=1.2\times10^6\ M^{-1}$). According to the

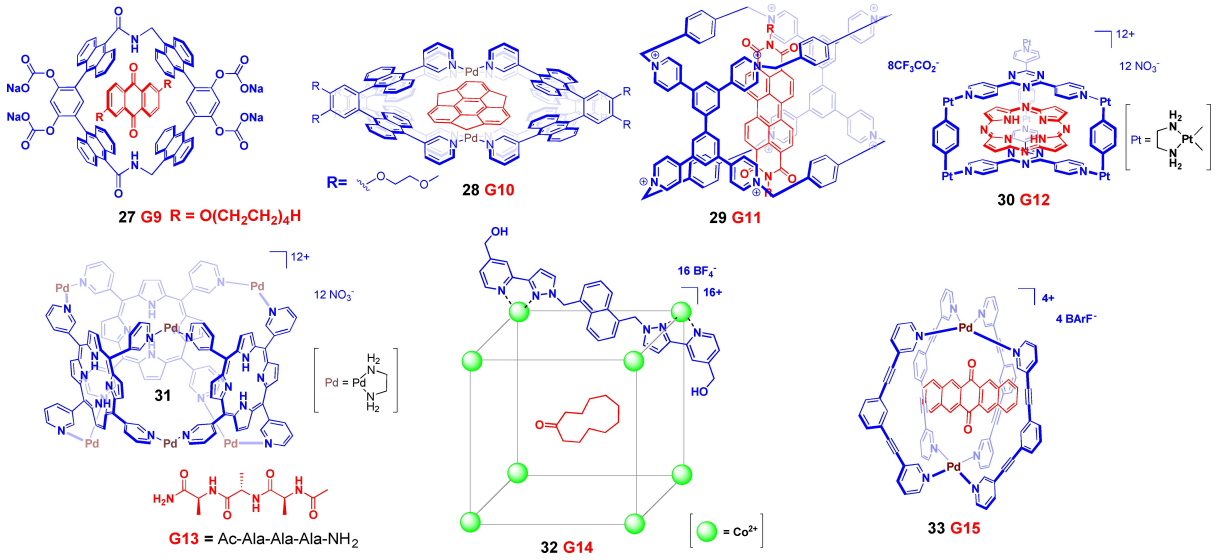

Figure 4. Structures of receptors for neutral organic compounds.

X-ray structure, the strong binding for this guest was also consistent with the 55 % Rebek's filling rule. The comparison of the affinities of three isomeric substituted cyclohexanones showed that the more eccentric shapes did not fit well in the symmetric cavity of the host. Linear ketones did not bind because they required additional energy for conformational reorganization. Thus, shape and size complementarity are essential factors for strong binding in confined spaces.[55] Similar investigations were conducted with the Pd^{II} cage **33** reported by Lusby.[56] The ability of the cationic cage to encapsulate neutral quinones was investigated in different solvents. The competition of the solvents for hydrogen bonding interactions and the nature of the cage's counter-anions were found to be very important in achieving high binding affinities. For instance, the complexes of anthraquinone and pentaquinone (**G15**) with the tetra-BArF salt of the cage in CD_2Cl_2 solution produced the highest affinities, $K_a = 5.0 \times 10^7\ M^{-1}$and $K_a = 8.0 \times 10^8\ M^{-1}$, respectively. For 1,4-cyclohexanone no binding affinity was detected. This work nicely illustrated the importance of the hydrogen bonding interactions that are maximized in non-polar solvents.

A series of aryl-extended calix[4]pyrroles were developed by the Ballester group to bind polar guests in organic and aqueous solutions (Figure 5). The cone conformation of the tetra-α-isomers of aryl-extended calix[4]pyrroles defines a deep and polar aromatic cavity that is open at one end and closed at the opposite one with four pyrrole NH groups. One of the exciting findings with receptor **34** was its ability to bind creatinine (**G16**) with an estimated binding affinity (K_a) of at least $10^7\ M^{-1}$ in CH_2Cl_2 solution. The crystal structure of the **G16**⊂**34** complex revealed the key intermolecular interactions of the complex and the host–guest complementarity: the creatinine oxygen atom was bound to the pyrrole-NH groups, and a hydrogen bonding interaction between the guest NH_2 group and the inwardly directed PO group was also formed. The receptor was used as an ionophore to construct a potentiometric sensor, *a.k.a.* ion selective electrode, able to detect creatinine in urine and blood plasma with high selectivity.[57]

In further studies, pyridine *N*-oxide derivatives were found to form thermodynamically and kinetically stable complexes with this type of calix[4]pyrroles.[58] Water-soluble receptors **35a**, **35b**,[59] and **36**[60] showed extremely high binding constants ($K_a = 10^5$–$10^9\ M^{-1}$) for **G17**–**G22** according to ITC experiments and NMR competitive binding studies. The guest molecules had different substituents at the *para*-position of the pyridine *N*-oxide knob and thus possessed different sizes of nonpolar surface areas. With this series of hydrophobic guests, it was possible to quantify the hydrophobic effect to binding, which was estimated to be in the order of 33–38 $cal\,mol^{-1}\,Å^{-2}$. The bridging of the aromatic cavity of an aryl-extended calix[4]pyrrole resembling the resorcin[4]arene upper rim led to unprecedented calix[4]pyrrole cavitands, i.e., **37**. Molecular modeling studies suggested that **37** could adopt vase and kite conformations in solution. However, experimentally only the kite conformation of **37** was observed both in the solution and the solid state. According to the results of ITC experiments, **37** bound **G17** with an association constant $K_a = 6.3 \times 10^7\ M^{-1}$ in $CHCl_3$. Apparently, size, shape, and functional group complementarity played a very important role in the stability of the **G17**⊂**37** complex.[61]

The strong interactions established between calix[4]pyrroles and pyridyl *N*-oxides allowed the authors to investigate the modulation of the binding affinity using several light-responsive receptors. For instance, receptor **38**, decorated with four azobenzene switching units, changed its cavity size upon light irradiation. Complexation studies of *N*-oxide **G17** and ion pair **G23** with and without light-irradiated samples of the receptor **38** supported that the *cis*-enriched isomers had a smaller aromatic cavity than the all-

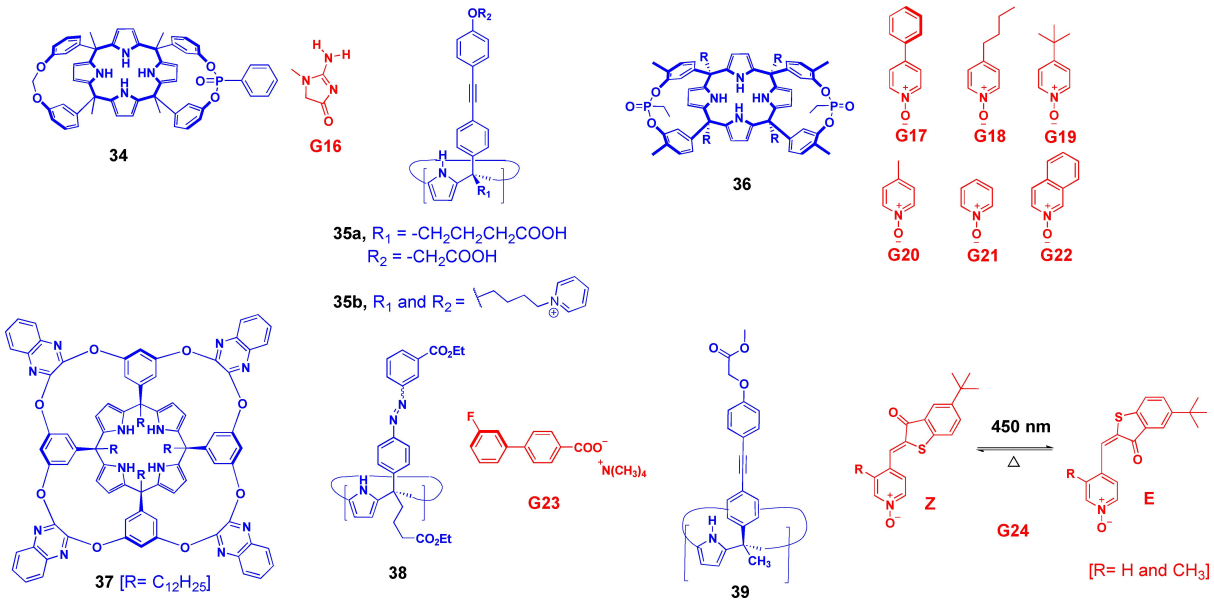

Figure 5. Molecular structures of calix[4]pyrrole-based receptors.

trans counterpart. The affinity of **38** for guests **G17** and **G23** changed significantly upon light-induced isomerization. That is, K_a(**G17**⊂all-*trans*-**38**) = $7 \times 10^6\ M^{-1}$ changed to K_a(**G17**⊂*cis*-enriched-**38**) = $0.5 \times 10^6\ M^{-1}$ and from $5.1 \times 10^6\ M^{-1}$ to $0.3 \times 10^6\ M^{-1}$ for the analogous complexes with **G23**.[62] A different situation was observed when the switchable guest **G24** was used in combination with a non-light responsive calix[4]pyrrole. The results of the ITC binding experiments of receptor **39** with **G24** in $CHCl_3$ solution showed a small difference (2.2–2.8-fold) in the binding affinities for the *Z*- and *E*- isomers of the guest. This finding suggested that the receptor's cavity adapts to the shape of the photo-switched guests.[63]

3. Positively Charged Guests

While coulombic and other electrostatic interactions drive the binding in organic solutions, the hydrophobic effect has a considerable contribution in water. Often the hosts for cationic guests are equipped with carboxylate or sulfonate groups warranting good solubility in water and an overall large negative charge. Such negatively charged hosts are pH-sensitive. There are also neutral receptors soluble in water that can efficiently coordinate positively charged guests through the hydrophobic effect and other electrostatic interactions, i.e., cation–π, CH–π, π–π etc. In contrast to the charged receptors, the neutral counterparts can bind the guests over a broad range of pH values.

An example of a negatively charged host is the water-soluble tetrasulfonated 1,5-dinaphtho-32-crown-8 (**40**) bearing four negative charges (Figure 6). Receptor **40** encapsulated dicationic bipyridiniums reaching a binding affinity of $K_a = 10^7\ M^{-1}$ for paraquat (**G25**).[64] According to the ITC results, the complexation processes were mainly driven by enthalpy (−27.20 to −43.92 kJ mol^{-1}). Although this thermodynamic signature is more commonly observed for the binding of certain hydrophobic neutral guests, that is the so-called "nonclassical hydrophobic effect", the formation of the **G25**⊂**40** complex was based on a different recognition process. The structure of host **40** displayed a low degree of preorganization in comparison with e.g. metallocages that bind neutral guests. Therefore, solvation/desolvation, dispersion interactions, and electrostatic forces were decisive for the strong binding of **G25**. Given this combination of intermolecular interactions, host **40** was tested for its ability to bind nicotinamide adenine dinucleotide (NAD^+). Surprisingly, the negatively charged host **40** was able to bind NAD^+ ($K_a = 2.23 \times 10^3\ M^{-1}$) despite the presence of two negatively charged phosphate groups in its structure. The phosphate groups were expected to engage in strong repulsive coulombic interactions with the negatively charged host. Nevertheless, the high dielectric constant of water and its hydrogen-bonding properties are known to play an important effect in shielding the charges.

The attachment of carboxylate groups to a pillar[6]arene core (**41**) was used by Huang and co-workers for the recognition of paraquat (**G25**) in water.[65] The combination of electrostatic and dispersion interactions with the hydrophobic effect provided a strong stabilization of the complex $K_a = 10^8\ M^{-1}$ in water solution. Host **41** is one of the best receptors for binding paraquat in water. It is known that paraquat is prone to form a toxic radical cation upon reduction. The authors demonstrated that the strong

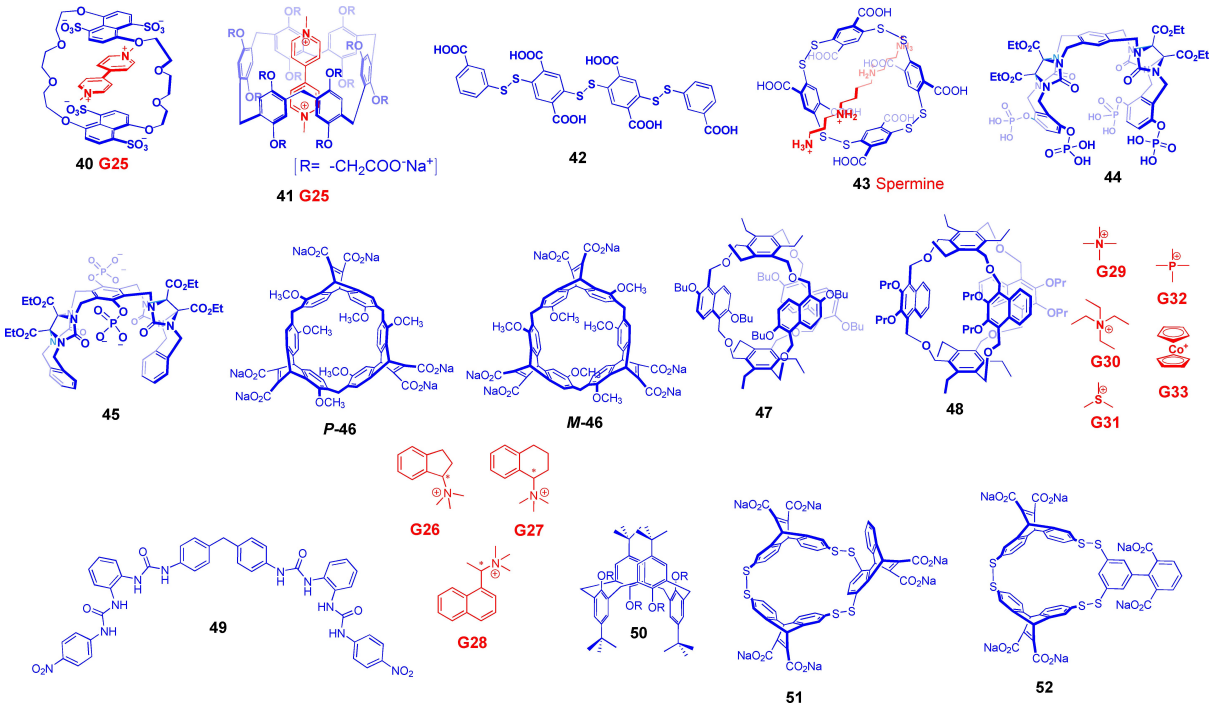

Figure 6. Receptors for positively charged guests.

encapsulation of paraquat in **41** led to a dramatic decrease in toxicity for cells.[65] Pillar[6]arene acted as a supramolecular protection in the reduction reaction of paraquat. Later on, it was found that 4,4′-diazoniastilbene was also encapsulated in the same host forming a 1:1 complex with high binding affinity: $K_a = 10^7\ M^{-1}$.[66] In this case, pillar[6]arene showed a photoprotective role for the encapsulated stilbene. *p*-Sulfonatocalix[4]arene also possesses a strong affinity for pyridinium fragments. For instance, Nau and co-workers reported the ability to form a strong complex with lucigenin in water ($K_a = 10^7\ M^{-1}$) and used the host–guest complex in the monitoring of membrane transport.[67]

A combinatorial approach to select a water-soluble receptor for spermine was presented by the Otto group. The amplified host represented a rare example of high-affinity binding resulting from its templated synthesis.[68] The building blocks of the receptor were oxidized under air and equilibrated at pH 8.25 to form disulfide (S–S) bonds between identical and different components. Compound **42** was the major component of the dynamic combinatorial library in the absence of spermine. The addition of spermine induced the amplification of macrocycle **43**. The affinity constant of **43** for spermine in water was determined to be $K_a = 4.5 \times 10^7\ M^{-1}$. NMR studies indicated that **43** formed a 1:1 complex with spermine displaying a [2]pseudorotaxane topology, in which spermine is threaded through the cavity of the host.

Tiefenbacher and co-workers studied the binding properties of a series of phosphorylated molecular tweezers using ^{1}H NMR titrations and various mono-, di-, and triamine guests, generally as the hydrochloride salts. In particular, they successfully constructed conformationally flexible glycoluril-derived molecular tweezers **44** and **45**. In unbuffered D_2O, spermine was bound to **44** and **45** with almost nanomolar affinity $K_a = 1.5 \times 10^8\ M^{-1}$ and $7.9 \times 10^6\ M^{-1}$, respectively.[69] Chen and Han recently reported on new octopus[3]arenes (*P*)-**46** and (*M*)-**46**, which have inherent chirality and exhibited enantioselective recognition of chiral amines. As in previously described receptors, (*P*)-**46** and (*M*)-**46** bear carboxylate groups for the establishment of coulombic interactions and a sizeable hydrophobic cavity. Chiral guests **G26–G28** were bound with $K_a = 10^6\ M^{-1}$ in water. The receptors successfully discriminated the binding of chiral amines with a *S*/*R* selectivity ratio of 12.[70]

Dialkoxynaphthalene-based macrocycles inspired researchers to design new cryptand naphthocages **47** and **48**.[71] The receptors showed high affinities ($K_a = 10^7$–$10^9\ M^{-1}$) for cations **G28–G33**, as determined by ITC experiments in dichloroethane/acetonitrile 1:1 solution. The highest affinity was measured for receptor **47** binding the cobaltocenium cation **G33**. The tetraethylammonium cation ($K_a = 3.7 \times 10^7\ M^{-1}$) was a slightly better guest than the tetramethylammonium analogue ($K_a = 1.6 \times 10^7\ M^{-1}$). The size of the guest was important in determining the selectivity of the cage for the binding of organic cations. According to ITC results, the binding process was strongly enthalpically favored. The formation of the complexes highlighted the important role played by cation–π and dispersion interactions in driving the binding event.

Ligand **49** was designed by Wu and co-workers and has a V-shaped spacer and two arms with urea motifs.[72] Tetramethylammonium phosphate templated the self-assembly of ligand **49** into a triple anion helicate featuring a hydrophobic cavity. The cavity of the self-assembled receptor resembled that of the protein binding site for choline. It was shaped by four benzyl rings, which are potential donor groups for cation–π interactions. Fluorescence displacement assays with 4-(4-dimethylaminostyryl)-1-methylpyridinium iodide as an indicator were employed to determine the binding constants of the self-assembled helicate with a series of guests. The dye formed a 1:1 complex with the supramolecular dianionic helicate host featuring a stability constant of $10^6\ M^{-1}$ in acetone/1.5 % H_2O. Among the four tested tetraalkylammonium guests (choline, acetylcholine, L-carnitine, and glycine betaine), choline was bound about 15-times stronger. Mechanistic studies showed that the binding of the trimethyl-alkylammonium head and the hydroxy group at the right distance were critical for the observed binding selectivity.

An interesting work describing the highly efficient binding of nitric oxide in CH_2Cl_2 solution using cation radicals of novel arene receptors was reported by Rosokha and Kochi.[73] This work represents a rare example of molecular recognition of a gas using synthetic hosts. The nitrosonium ion was found to spontaneously form charge transfer complexes with aromatic donors. The strong binding arises from the donor–acceptor interaction, i.e., the formation of a charge transfer complex. Notably, the binding of nitric oxide to the radical cation of the arenes produced the same cationic charge transfer complex owing to the following coupled equilibrium:

$$ArH + NO^+ \rightleftharpoons [ArH \cdots NO]^+ \rightleftharpoons ArH^+ \cdot + NO\cdot \qquad (1)$$

The authors discovered that 2:1 complexes were formed at high concentrations of the arenes, and X-ray crystallography assigned the complexes a sandwich structure. The unusual co-facial arrangement of the 2:1 complexes made the authors connect their binding geometry with that of the diarene ligands (hosts) optimized for the chelate effect. The radical cations of the diarene guests were effective in producing the ditopic binding of nitric oxide. The addition of several diarene ligands to a dilute CH_2Cl_2 solution of the nitrosonium cation produced the immediate observation of purple colorations. Among the studied diarenes, an extraordinary binding affinity was determined for the 1,3-alternate conformation of the simple calix[4]arene **50**: $K_a = 2.0 \times 10^8\ M^{-1}$. The analysis of the binding properties of the different diarene receptors revealed a linear relationship between the free energy of binding and the oxidation potential of the arene donors. Importantly, considering the three-state equilibrium described above, weak arene donors ($E_{ox} > 1.5$ V) favored the diamagnetic reagents (ArH and NO^+). Conversely, electron-rich donors ($E_{ox} < 1.5$ V) shift the equilibrium to the paramagnetic species ($ArH^{\bullet+} + NO^{\bullet}$)

and the CT complex was only observed at low temperatures. The formation of the CT complex is optimized for E^0_{ox}(arene) $\approx E^0_{red}(NO^+) = 1.5$ V vs SCE.

Recently, post-translationally modified (PTM) amino acids have gained attention as targets for supramolecular recognition using synthetic receptors. Some PTM proteins are also related to health and disease i.e., cancer. Hof and co-workers reported a series of sulfonated calix[4]arenes that bind selectively and with high affinity ($K_a > 10^6\ M^{-1}$) to PTM histones possessing trimethyllysine residues. PTM histones play an important role in gene regulation and oncogenesis.[74] Cation–π interactions and the hydrophobic effect were postulated as the main driving forces of the strong binding detected in water solution. A different design approach was exploited by the Waters group in the selective binding of methylated lysine residues. The authors selected macrocyclic receptors through a dynamic combinatorial approach. For instance, receptor **51** bound *N*-trimethyllysine (Kme3) with a $K_a = 3.3 \times 10^6\ M^{-1}$ in a buffered water solution. The binding selectivity for Kme3 over Kme2 (*N*-dimethyllysine) was 14-fold.[75] Remarkably, with the help of receptor **52** it was possible to revert the selectivity for Kme3 to Kme2 (Figure 6). The latter receptor was also amplified from a dynamic combinatorial library and bound Kme2 in the peptide sequence Ac–WGGGQTARKme2STG–NH_2 with a $K_a = 5.0 \times 10^6\ M^{-1}$.[76]

4. Negatively Charged Guests

Azacrowns are classical supramolecular hosts for anions. They bear multiple positive charges in neutral or acidic aqueous solutions and bind anions via multiple coulombic and hydrogen bonding interactions. In the majority of cases, their binding affinities for 1:1 complexes with inorganic anions exceed $10^6\ M^{-1}$. As expected, in basic media, the azacrowns display a reduced number of positive charges; hence, their affinities for a particular anion drop dramatically.[77] There are several reviews describing these types of receptors. For this reason, we mention below only the most selective azacrown receptors. Among the hexa-azacryptands known to date, **53a** and **53b** (in their fully protonated state) demonstrated the highest binding affinities for tetrahedral anions such as SeO_4^{2-} and $S_2O_4^{2-}$ and oxalate with K_a values $> 10^7\ M^{-1}$ for the 1:1 complexes (Figure 7). Interestingly, **53b** was even able to bind the CrO_4^{2-} anion. Under the experimental conditions (pH ≈ 3) used for the K_a determination, the anion was present in its mono-protonated form, $HCrO_4^-$ ($pK_a = 6.49$). However, absorption spectroscopy revealed that the anion was complexed in its chromate form (dinegative). In short, the electrostatic driving force of binding favors the dinegatively charged form of the anion upon complex formation. The Steed group reported high selectivity for fluoride ($> 10^5$) in the binding of halides with receptor **54**.[78] The binding affinities of the hexaprotonated form of host **54** for fluoride and chloride measured using potentiometric pH titrations were $K_a = 8.7 \times 10^9\ M^{-1}$ and $1.5 \times 10^4\ M^{-1}$, respectively. Most likely, the conformational rigidity of these highly charged hosts is essential for achieving the observed selectivity. For instance, previously developed octa-azacryptands **53** and bis(tren) cryptands **55** showed a reduced selectivity in the binding of the halide series.[79] Dye-functionalized cryptands **56** and **57** were recently investigated in the Kataev group as fluorescent sensors for anions in an aqueous buffered solution. The introduction of anthracene or naphthalimide units allowed the detection of the anions via a "turn-on" fluorescence mechanism. It was shown that the receptors at pH 3.6 are at least 5-fold protonated and can bind sulfate, oxalate, and pyrophosphate anions with binding affinities on the order of $10^6\ M^{-1}$ or even higher.[80] The driving force of such strong binding is derived from the five to six possible coulombic attractive interactions that are established between the

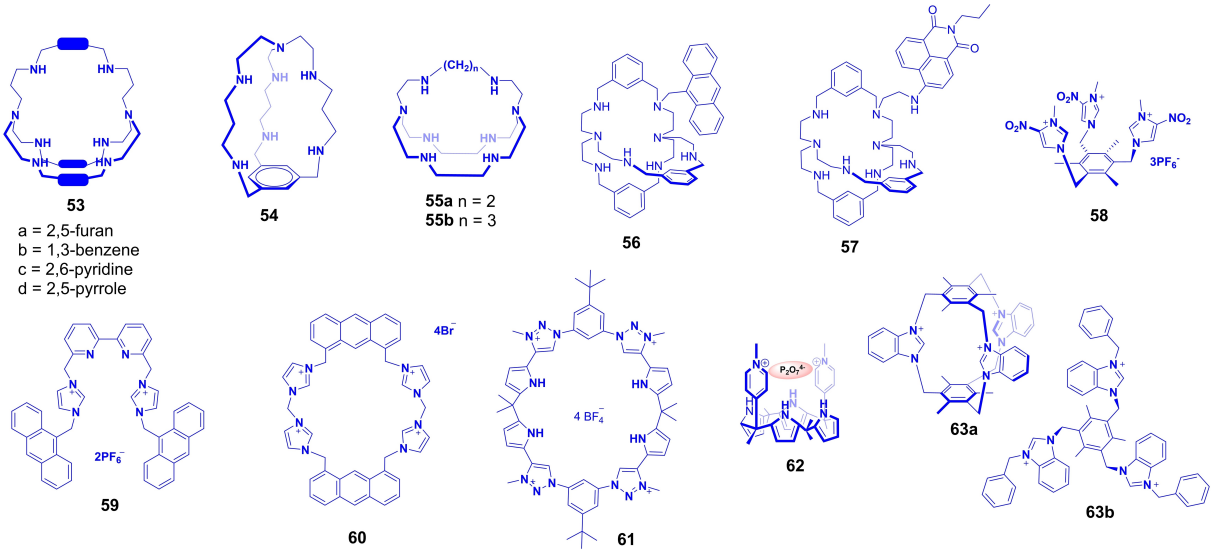

Figure 7. Structures of synthetic receptors for anions.

encapsulated anion (dinegatively charged) and the ammonium sites of the multiple positively charged receptor.

In analogy to the azamacrocyclic receptors, imidazolium-based receptors bearing a pH-independent positive charge were extensively investigated for anion recognition. They can form imidazolium C–H···O hydrogen bonds that appear to be highly efficient in organic and aqueous solutions. For instance, receptor **58**[81] is an interesting example[82] because its binding properties were investigated in different solvent mixtures. The receptor had a binding affinity for chloride of $10^6\,M^{-1}$ in acetonitrile solution containing 10% DMSO. Remarkably, the binding stability of the complex diminished to $110\,M^{-1}$ in pure DMSO. This result is a striking example showing that the highly polar and hydrogen-bonding competitive DMSO dramatically diminished the association constant via strong solvation of the three imidazolium binding units of the receptor. This finding is also consistent with the high binding constant ($6.2\times10^6\,M^{-1}$) determined for the complexation of pyrophosphate with receptor **59** in pure acetonitrile solution .[83] A good correlation was found between the Hofmeister series for anions and the binding constants of a receptor that differentiated dihydrogen phosphate and monohydrogen sulfate anions.[84] The authors pointed out that these results were also consistent with the rule stating that a receptor with a large number of hydrogen bond donors favorably binds anions with the greater number of hydrogen bond acceptors. Receptor **60** was also designed by combining imidazolium binding units with aromatic spacers and possessed a higher overall positive charge than **59** (2+ vs 4+). This makes receptor **60** a better fit for triphosphate nucleotides since they are triply negatively charged. Thus, receptor **60** is considered one of the best hosts for the binding of guanosine triphosphate (GTP, $K_a=10^6\,M^{-1}$) in a buffered aqueous solution.[85] Sessler and co-workers followed a similar strategy in the design of the triazolium macrocyclic receptor **61.**[86] The receptor combines triazolium units $(CH)^+$ with pyrrole (NH) binding sites, which work together to coordinate anionic species. Similarly to the above-described examples, the receptor binds pyrophosphate and hydrogen sulfate with affinities exceeding $10^6\,M^{-1}$ in both acetonitrile and methanol solutions. A better selectivity for pyrophosphate binding was achieved with the calix[4]pyrrole-based receptor **62** functionalized with pyridinium units. According to UV/Vis studies, it bound pyrophosphate in acetonitrile solution with a $K_a=2.5\times10^7\,M^{-1}$. The binding affinity did not drop much in an acetonitrile/30% water mixture: $K_a=3.6\times10^6\,M^{-1}$. However, for the most strongly competing fluoride anion, the binding affinity of the receptor in the presence of water decreased significantly: from $6.9\times10^6\,M^{-1}$ in pure acetonitrile to $2.5\times10^4\,M^{-1}$ in a 30% water/acetonitrile solvent mixture.[87]

An interesting cage-like host **63a** with a relatively small inner cavity for fluoride binding was reported by Amendola and co-workers.[88] The stability constant of the 1:1 complex of F^- with **63a** was estimated to be larger than $10^7\,M^{-1}$using UV/Vis titrations in acetonitrile solution. Larger anions such as chloride, bromide, and nitrate did not fit in the cavity of the receptor. Interestingly, the benzimidazolium-based receptor demonstrated a stronger affinity than the one published earlier by the same group, also incorporating imidazolium binding sites in an acyclic tripodal scaffold (**63b**). Thus, it was suggested that steric effects and geometric constraints were determining factors for achieving high selectivity and affinity in the binding of such small mono-atomic anions.

Considering phosphate and sulfate binding in an aqueous solution, one of the highest affinities obtained for synthetic organic receptors corresponds to the positively charged pyrrole-based cryptand **53d**. Calorimetric measurements were performed by Grell et al. to study anion binding at different pH values.[89] Importantly, the determined association constants were greater than $10^6\,M^{-1}$ for the phosphate and sulfate ions. However, the binding strength was strongly dependent on pH and ionic strength. The binding events were mainly driven by enthalpy and partially opposed by entropy. The unfavorable entropy contributions were explained by the co-encapsulation of water together with the bound anion in the cryptand's cavity.

Focusing on sulfate recognition, the Kubik group designed one of the strongest binding receptors. In collaboration with the Otto group and using a dynamic combinatorial approach, receptors **64a** and **64b** were discovered (Figure 8). The receptors showed very high stability constants for the 1:1 complexes with sulfate in a CH_3CN/H_2O 1:1 solvent mixture ($K_a=4.7\times10^8\,M^{-1}$ for **64a** and $3.8\times10^7\,M^{-1}$ for **64b**).[90] The X-ray crystal structure of the $SO_4^{2-}\subset$**64a** complex revealed intramolecular contacts between the nonpolar regions of the proline residues of the macrocycles. Notably, although these contacts were not directly involved with the anion binding, they appeared to play a significant role in the stabilization of the complex. The fact that increasing the water content in the mixture had a reduced effect on the binding constant values fully supported this conclusion.[91] Additional binding experiments with a monomeric cyclopeptide macrocycle also supported the involvement of intramolecular macrocycle–macrocycle interactions because a 1:2 anion-receptor complex was observed in this case. Likewise, in DMSO solution, the nonpolar interactions between the two macrocycles did not take place (the hydrophobic effect is not operative), and instead of 1:1 binding, only a 2:1 anion-receptor complex was observed. Finally, the introduction of hydrophilic OH groups on the proline residues of the monomeric cyclopeptide caused the exclusive formation of 1:1 complexes even in an aqueous solution. This example represents a very attractive strategy to reinforce host–guest interactions by designing a host structure featuring intra-receptor nonpolar interactions (hydrophobic effect). This makes the binding event less dependent on the increase of solvent polarity by reinforcing the latter interactions.[92]

Another efficient macrocyclic receptor based on rigid thiourea fragments was reported by Wang and co-workers. Macrocyclic host **65** is able to capture the ethanedisulfonate dianion with a binding constant of $2.1\times10^6\,M^{-1}$ determined using ITC experiments.[93] An interesting application of this strongly binding host was its use in tuning the catalysis of the Povarov reaction using ethanedisulfonic acid. The tight trapping of the dianion by the macrocycle favored imine

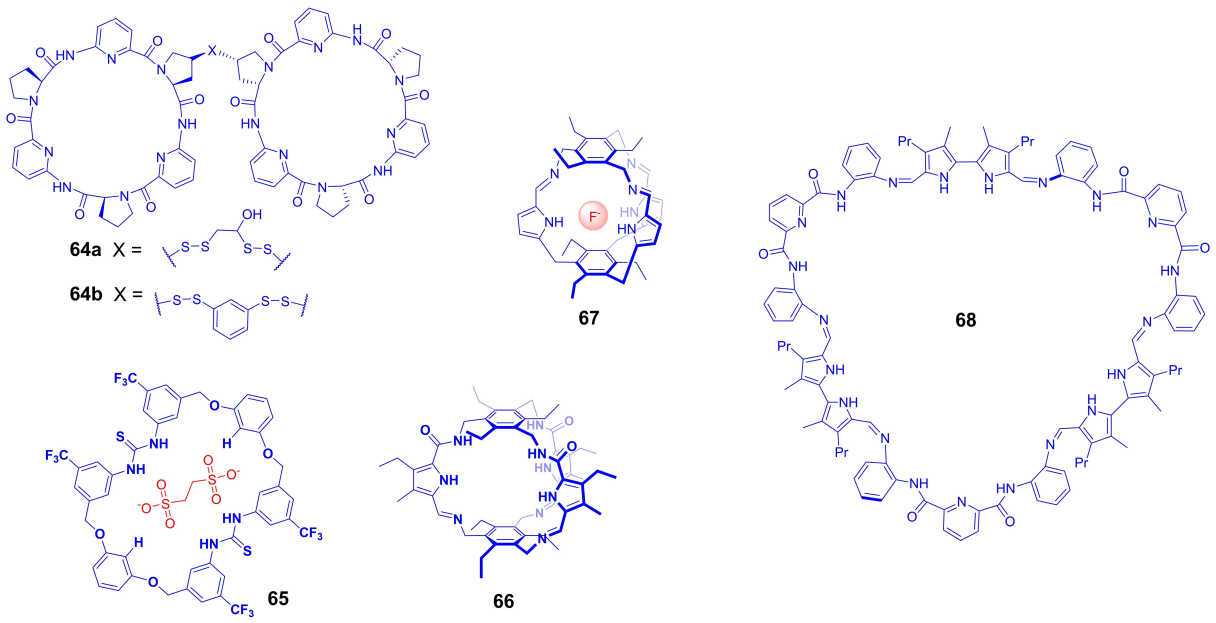

Figure 8. Structures of synthetic receptors for anions.

protonation and the subsequent acid-catalyzed reaction. Other acyclic analogs showed a diminished effect. Several molecular cages encapsulating inorganic anions were developed by the Sessler group. For instance, cage **66** combines imine binding sites as hydrogen bond acceptors and amido-pyrrole units as hydrogen bond donors. Fluoride, sulfate, hydrogen sulfate, dihydrogen phosphate, and hydrogen pyrophosphate anions displayed binding affinities (K_a) on the order of $10^6\ M^{-1}$. The increase in the charge of the anions did not significantly affect the binding strength.[94] For instance, the affinities of the cage for SO_4^{2-} and $HP_2O_7^{3-}$ were $K_a = 2.7\times10^6\ M^{-1}$ and $1.8\times10^6\ M^{-1}$, respectively. The reduction in the size of the macrocycle, by replacing the methylene amide spacers by methylene units, yielded receptor **67**, which showed an improved binding selectivity for fluoride ($K_a = 10^7\ M^{-1}$) in chloroform and DMSO solutions.[95]

The 3D arrangement of binding sites to coordinate phosphate and sulfate anions was achieved by the Kataev group through templated amplification of a dynamic combinatorial library.[96] A pyrrole-based dialdehyde and a pyridine-based diamine were condensed in a [3+3] reaction to form the large macrocycle **68**. The macrocycle was able to wrap the phosphate anion in an acetonitrile solution forming a complementary polar cavity. In sum, 12 hydrogen bonds stabilized the binding of the anion in the cavity of **68** giving rise to an extraordinarily high affinity. According to the results of UV/Vis spectroscopy titrations with different inorganic anions, the highest affinities were measured for sulfate and phosphate with binding constants $K_a = 9.7\times10^6\ M^{-1}$ and $5.5\times10^6\ M^{-1}$, respectively. An interesting feature of receptor **68** was that the 12 hydrogen bonds provided in the binding of phosphate coincide with the hydrogen bonds found in the phosphate binding protein complex.

Borate anions have a hydrophobic nature suitable for interaction with hydrophobic cavities. For instance, a very strong binding interaction of γ-cyclodextrin (γ-CD) was observed by Nau and co-workers with boron clusters in an aqueous solution.[97] According to the results of ITC experiments, the association constant of γ-CD with the $B_{21}H_{18}^-$ cluster is $K_a = 1.8\times10^6\ M^{-1}$. This magnitude represents one of the largest binding constants measured for 1:1 complexes of CDs. However, it is slightly smaller than the binding affinity of γ-CD for *meta*-COSAN, $Co(C_2B_9H_{11})_2^-$ ($K_a = 3\times10^6\ M^{-1}$). Detailed experimental and theoretical investigations suggested that the main driving force for the complex formation was the small desolvation penalty required for the inclusion of the clusters in the CDs' cavities. The formation of the host–guest complex was explained to be driven by the so-called chaotropic effect, which describes the strong interaction of large and polarizable anions that are weakly solvated with the hydrophobic inner cavity of suitable hosts.[98]

A simple and elegant approach to increase binding affinity to micromolar level was realized by Petter et al. by placing two β-cyclodextrin units in close proximity by means of a disulfide bond (S–S bridge). In this way, the authors achieved extraordinary binding affinities for the complexation of dyes such as methyl orange (MO, $K_a = 5.8\times10^5\ M^{-1}$) and ethyl orange (EO, $K_a = 2.0\times10^6\ M^{-1}$) in water carbonate buffer at pH 10.5.[99] The dyes contained two phenyl rings in their scaffolds and established a ditopic interaction with the receptor by including a phenyl group in each one of two cyclodextrin units of the receptor (chelate or multivalent cooperativity). When compared to the coordination strength provided by the inclusion of a single phenyl ring into a cyclodextrin unit, the ditopic interaction of the dyes with the receptor was responsible for a boost of up to 200-fold in the association constant values of the complexes.[100]

Guo et al. designed calix[5]arene **69** having five guanidinium appended units (Figure 9). The prepared receptor was employed in the encapsulation of a series of anionic guests. Using an indicator displacement assay (IDA) with fluorescein, the authors determined that **69** displayed binding affinities $>10^7\ M^{-1}$ for the binding of perfluorinated pollutants **G34** and **G35**. The authors also extended the use of the IDA in the selective detection of pollutants in tap and lake waters. Nanoparticles functionalized with a derivative of receptor **69** were used for the efficient removal of the pollutants from water via a magnetic absorption and filtration methodology.[101] An IDA with fluorescein and the water-soluble guanidinium-modified calix[5]arene **69** was also used in the detection of the cancer biomarker lysophosphatidic acid (**G36**).[102] The stability of the host–guest complex **G36**⊂**69** ($K_a = 1.6\times10^8\ M^{-1}$) was even higher than that of the 1:1 complexes of the previously investigated pollutants. It was also observed that other dyes (**G37–G39**) formed highly stable inclusion complexes with **69**. The association constants for nearly all the 1:1 complexes of the latter dyes with **69** were in the range of 10^6–$10^8\ M^{-1}$.[103]

Kraus and co-workers explored the binding properties of the highly charged *per*-6-amino-ß-cyclodextrin in an aqueous buffer solution. Owing to the multiple positive charges of the receptor, it formed highly stable complexes with nucleotides, e.g., ATP, with a binding constant value of $K_a = 2.0\times10^7\ M^{-1}$. The authors used this high-affinity binding for the design of an artificial and selective carrier capable of transporting natural and synthetic triphosphates. The receptor was conjugated to a cell-penetrating agent that translocated the complex of the triphosphate derivative across the membrane. The authors showed the successful metabolic labeling of DNA through the transport of fluorescently labeled triphosphates into eukaryotic cells and bacteria.[104]

The recognition of the biologically important ATP under neutral pH was profoundly studied in the pioneering work of Lehn and Kimura. Highly charged anionic guests, like citrate, ATP, $Co(CN)_6^{3-}$, and $Fe(CN)_6^{4-}$ were bound in an aqueous medium by polyammonium macrocycles with association constants (K_a) in the range of 10^6–$10^9\ M^{-1}$.[105] A careful analysis of the ^1H NMR spectra of the 1:1 complex of the macrocyclic host with ATP revealed the simultaneous interactions of the nucleobase and the phosphate residue with the azacrowns.[106] To increase the affinity of the receptors for the nucleotides, it was proposed to introduce acridine moieties to the polyammonium macrocyclic scaffold (**70**).[107] Macrocycle **70**, possessing two acridine moieties, adopted a folded structure that quenched its fluorescence. However, upon guest binding, the structure of the bound host rearranged with the observation of a concomitant fluorescence enhancement. According to the results of potentiometric pH titrations, **70** bound ATP and NADPH in a water solution with very high association constants, $K_a = 7.0\times10^7\ M^{-1}$ and $3.0\times10^8\ M^{-1}$, respectively. A more rigid host was designed by positioning two *cis*-oriented phenanthridinium units parallel one to another (**71**).[108] The preorganization effect of the cyclic host allowed the inclusion of various nucleotides in its aromatic cleft with affinities in the range of 10^5–$10^6\ M^{-1}$.

The Inouye group reported an elegant design of pyrene-based cyclophanes able to encapsulate aromatic guests in water. The presence of two parallel pyrene units allowed the binding of large aromatic guests.[109] Binding studies with neutral, positively, and negatively charged guests were carried out in water/ethylene glycol (3:1) solvent mixtures using UV titrations. For instance, the association constants of **72** with ATP and with 3-hydroxy-2,7-naphthalenedisulfonic acid disodium salt (**G40**) provided the highest association constant values on the order of $10^6\ M^{-1}$.

A remarkably strong coordination of chloride is exerted by the calix[4]bipyrrole receptor **73** (Figure 10). The polypyrrole receptor **73** is neutral but bound chloride with an association constant of $2.9\times10^6\ M^{-1}$ in acetonitrile solution. The receptor also displayed an extraordinary selectivity for chloride binding: 26-fold over bromide and 51000-fold over iodide.[110] The encapsulation of halide ions was also explored using highly positively charged coordination complexes possessing catenated and knot structures. Leigh and

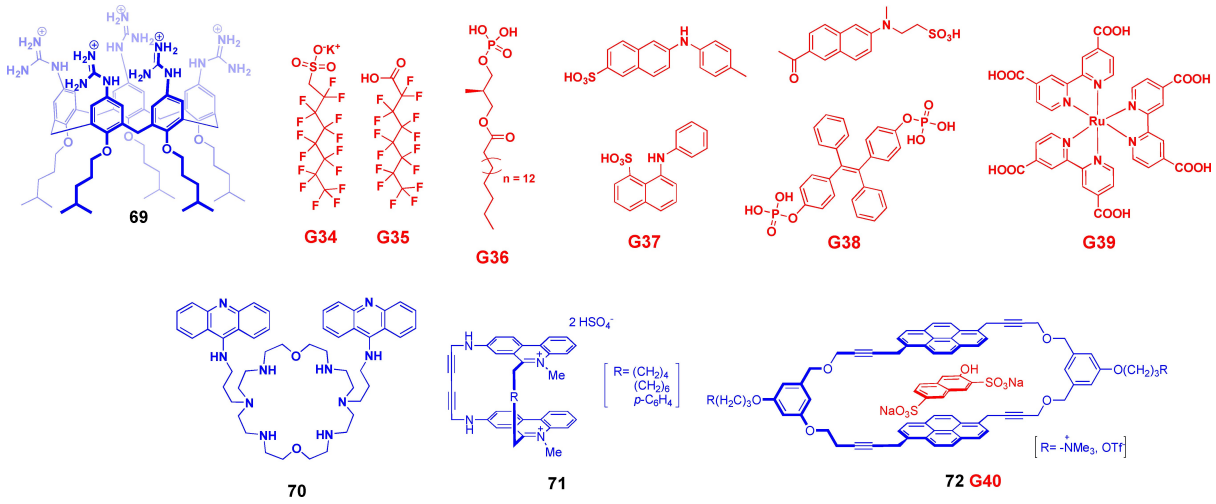

Figure 9. Structures of the synthetic receptors employed for the binding of anionic species.

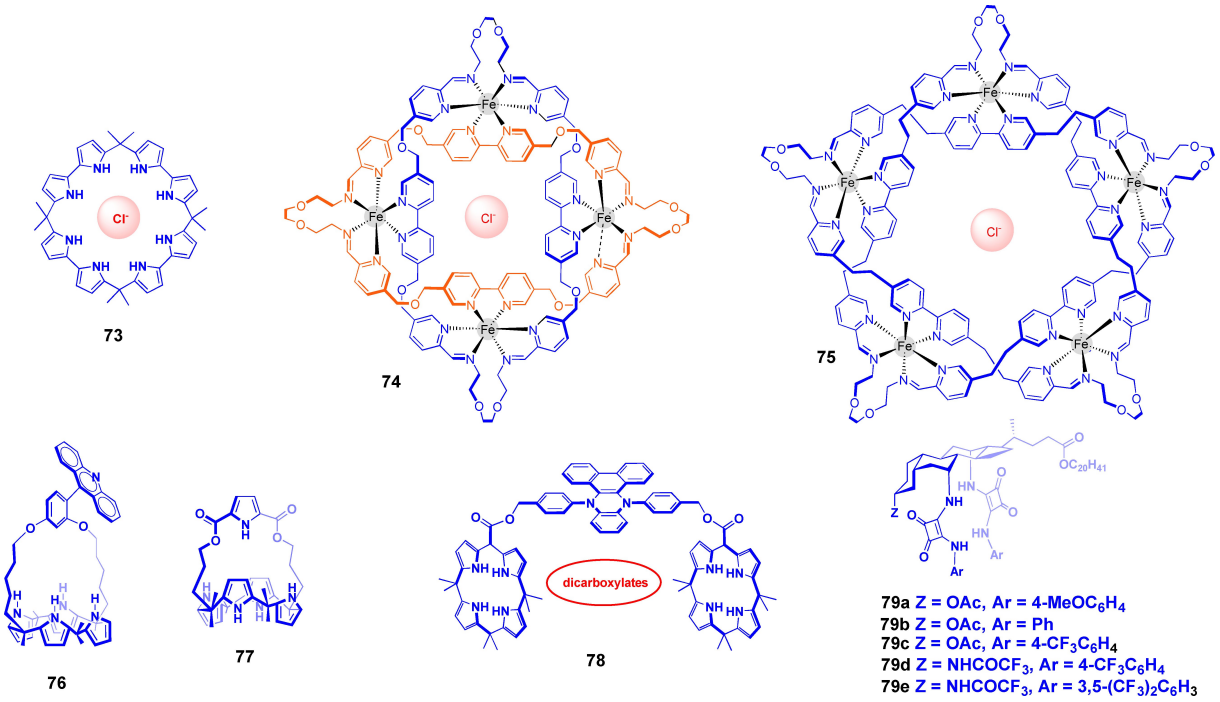

Figure 10. Structures of receptors for anions.

co-workers synthesized a Fe^{II}-based trefoil knot and catenane architectures capable of binding Cl^-, Br^-, and I^- via noncovalent C–H···X interactions. The association constants for the anion binding determined in acetonitrile solution were extremely high. In particular, those for the chloride and bromide anions ranged from 10^8 to $10^{10}\,M^{-1}$. To accurately determine such large binding constants, ^1H NMR titration experiments involving competitive methods were used.[111] As a competitive receptor, the authors used calix[4]bipyrrole **73**. The binding constants of the 1:1 complexes of **74** and **75** with chloride were calculated as $K_a = 3.6 \times 10^{10}\,M^{-1}$ and $K_a = 1.7 \times 10^{10}\,M^{-1}$, respectively.

The Lee group proposed an approach to design an even better receptor for chloride binding. The idea was to strap a calix[4]pyrrole scaffold with an additional bridging spacer to generate a three-dimensional cavity. The synthesized strapped calix[4]pyrrole **76** was employed for the encapsulation of halide ions, especially Cl^- and Br^-.[112] The appropriate preorganization of the receptor's scaffold produced a high association constant for the 1:1 complex with chloride in acetonitrile ($K_a = 2.4 \times 10^7\,M^{-1}$ using ITC). Continuing with this design strategy, the Sessler group also reported a series of unprecedented strapped calix[4]pyrroles having a variable bridging spacer.[113] The pyrrole-based strapped macrocycle **77** showed the highest binding constant for chloride in acetonitrile, $K_a = 1.8 \times 10^7\,M^{-1}$. Apparently, this is due to the presence of an additional pyrrole N–H hydrogen bond donor site in the strapped calix[4]pyrrole structure. An alternative design to build high-affinity calix[4]pyrrole-based receptors consisted of covalently connecting two units through a fluorescent phenazine spacer, as shown in receptor **78**. This receptor was able to coordinate dicarboxylates in acetonitrile solution with binding affinities reaching $10^7\,M^{-1}$.[114] The rigid phenazine spacer enabled fluorescence detection of the binding event and the differentiation between dicarboxylates owing to the different emissive properties of the formed complexes. A unique property of this design arose from the adjustment of the receptor conformation to the size of the guests which was reflected by the emission wavelength. According to the results of the fluorescence titrations with a series of tetrabutylammonium salts of α,ω-alkyldicarboxylic acids, the strongest binding of **78** was measured for C7 and C8 dicarboxylic acids ($K_a = 5.0 \times 10^7\,M^{-1}$ and $1.9 \times 10^7\,M^{-1}$) and for the aromatic isophthalic acid ($K_a = 5.7 \times 10^7\,M^{-1}$). A cleft-like design was also realized with a steroid-based receptor, **79**, which had axially oriented squaramide units.[115] According to the results of extraction experiments, the determined binding affinities were in the range 10^{10}–$10^{14}\,M^{-1}$. The receptors were also able to facilitate the transport of the anions through the membranes of unilamellar vesicles.

Flood and co-workers introduced the "triazolophane" macrocyclic receptors **80** for the binding of chloride in organic solvents with high affinity (Figure 11).[116] The receptor possesses only CH-hydrogen bonding donor sites that are adequately directed to interact with a chloride anion included in its cavity. Moreover, receptor **80** is highly rigid and has size complementarity to chloride. The authors conducted fundamental investigations on the relationship between the strength of the anion binding and the nature of the solvent (dielectric constant).[117] Receptor **80** coordinated Cl^- ions with exceptionally high affinity in various organic solvents producing 1:1 and 2:1 receptor–chloride complexes. Increasing the dielectric constant of the solvent

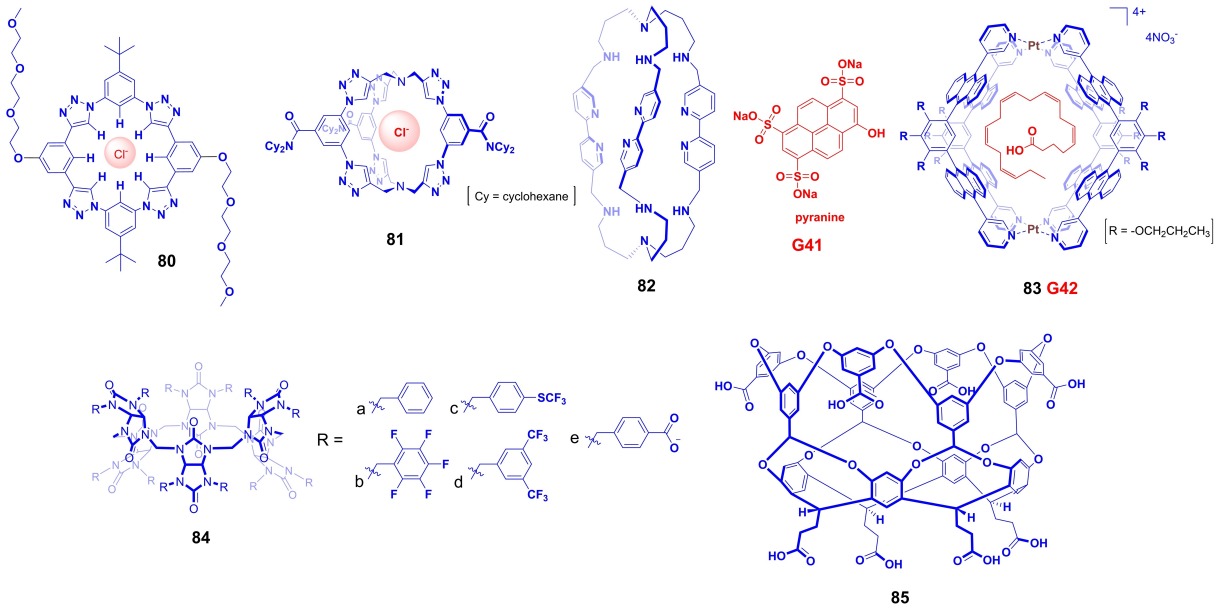

Figure 11. Structures of the synthetic receptors employed for anion binding.

produced a systematic drop in the binding affinity of the 1:1 and 2:1 complexes. Notably, the highest binding constant determined using UV/Vis titration experiments for the 1:1 complex was on the order of $10^{10}\,M^{-1}$ ($CHCl_3$). In the same solvent, the equilibrium constant for the formation of the 2:1 complexes from the 1:1 counterparts was larger than $10^8\,M^{-1}$. In DMSO water mixtures, the formation of the 2:1 complex showed binding cooperativity. This finding hinted to the existence of hydrophophic interactions between the two bound receptors, as observed for the macrocyclic peptide receptors developed by Kubik. In a later work, the Flood group reported the six-triazole-containing macrobicyclic receptor **81**.[118] The cage receptor **81** captured one Cl^- ion inside its ideally preorganized cavity via multiple CH-bonding interactions. The structure of the host–guest $Cl^-\subset$**81** complex in the solid state was revealed by X-ray analysis of a single crystal. The binding constant for the encapsulation of chloride was determined to be as large as $10^{17}\,M^{-1}$ in dichloromethane solution.

A series of positively charged covalent cages were shown to encapsulate one or more anions inside their cavities. An interesting case was reported by the Nitschke group for the encapsulation of various aromatic sulfonates in an aqueous solution.[119] The preorganized aromatic cavity and the cationic polyamine binding pockets of cage **82** were suitable for the inclusion of the investigated guests via a combination of π–π stacking and electrostatic (coulombic) interactions. Pyranine, **G41**, a membrane-impermeable fluorescent pH indicator containing one pyrene moiety and three sulfonate groups, was included in the cavity of **82** with an association constant of $K_a = 8.3\times10^8\,M^{-1}$ in water solution. The polyaromatic Pt^{II} metallo-cage **83** was reported to encapsulate natural unsaturated fatty acids in water.[120] While these fatty acids are rarely considered as guests for artificial receptors, the polyaromatic cage **83** was able to include them in its cavity in an aqueous medium forming highly stable 1:1 complexes. For example, polyunsaturated eicosapentaenoic acid (**G42**) showed the highest affinity ($K_a = 2.6\times10^6\,M^{-1}$) for **83** among the investigated guest series. Multiple CH–π/π–π interactions between the polyaromatic cage and the unsaturated fatty acid guests stabilized the host–guest complex. Most likely, the guest adopted a coiled conformation upon inclusion in the receptor's cavity.

Sindelar and co-workers developed a family of receptors known as bambusurils. Initially, receptor **84a** was found to encapsulate spherical halides in a chloroform solution with very high binding constants. In particular, the reported binding constant values for Br^- and I^- were $3.0\times10^8\,M^{-1}$ and $3.8\times10^9\,M^{-1}$, respectively.[121] The authors further functionalized the receptor's scaffold with outer rim carboxylic acid groups to warrant water solubility to the **84e** derivative in basic media.[122] This host was highly effective in binding weakly coordinating anionic guests, such as BF_4^- and PF_6^- anions, forming 1:1 complexes with stability constants higher than $10^6\,M^{-1}$. A possible reason for such high binding affinities is derived from the hydrophobic nature of the anions. The thermodynamic signature of binding was similar to that observed in the binding processes of cucurbiturils featuring the release of "high-energy" water molecules to the bulk solution. I^- and ClO_4^- displayed even higher association constants in the formation of 1:1 complexes with **84e** ($K_a = 1.0\times10^7\,M^{-1}$ and $5.5\times10^7\,M^{-1}$, respectively) than those of the BF_4^- and PF_6^- anions described above. Octaacid **85** possesses a hydrophobic concave surface that showed strong binding for adamantane carboxylic acid in water ($4.8\times10^6\,M^{-1}$), its bromo derivative ($K_a = 7.4\times10^6\,M^{-1}$),[123] and the adamantyl trimethylammonium cation ($K_a = 1.1\times10^6\,M^{-1}$).[124] The binding process of the carboxylic acid derivative is enthalpically driven: $\Delta H = -35.9\,kJ\,mol^{-1}$, $\Delta S = 6.8\,kJ\,mol^{-1}$. Interestingly, in the presence of 100 mM

$NaClO_4$, the thermodynamic signature was dramatically changed: $K_a = 7.7 \times 10^5\ M^{-1}$, $\Delta H = 3.3\ kJ\,mol^{-1}$, $\Delta S = 123.8\ kJ\,mol^{-1}$. The determined binding affinity of the perchlorate anion for **85** ($95\ M^{-1}$) is much lower than that of adamantane carboxylic acid. However, its presence plays a significant effect in the thermodynamic constants of the binding process. Binding studies involving "chaotropic" or "salting-in" anions are essential in understanding their effect in the unfolding and solubilization of proteins (Hofmeister effect).

5. Determination of Binding Constants

Stability constants can be determined using different methods and spectroscopies. Each methodology has its own limit for the accurate determination of binding constant values. This limitation is related to the minimum and maximum concentrations of the binding species that can be precisely determined using the selected titration methodology. For instance, in ^1H NMR spectroscopy titrations, $10^4\ M^{-1}$ is usually considered the limit of the association constant values that can be accurately determined using the technique. This limit is simply determined by the sensitivity of the ^1H NMR spectroscopy to concentration, which forces the use of at least mM concentrations. At this concentration and for a 1:1 complex, any binding constant value larger than $10^4\ M^{-1}$ will produce the saturation of the spectroscopic changes caused by the complex formation when an equimolar ratio of host and guest is reached. An accurate determination of a binding constant larger than $10^4\ M^{-1}$ will require working under more dilute conditions, which is unfeasible owing to the detection limit of the ^1H NMR spectroscopy technique. However, as shown in many cases for cucurbiturils, ^1H NMR spectroscopy is a useful method to measure binding constants on the order of $10^6\ M^{-1}$ and higher using competitive displacement binding assays. Isothermal titration calorimetry (ITC) experiments can be performed at concentrations similar to NMR or even lower, assuming that the heat released or absorbed per injection during the titration is sufficient to be measured accurately by the calorimeter (≈ 1 μcal for a 1 mL cell calorimeter). The integrated and normalized heat data of each injection (binding isotherm) is analyzed using an appropriate theoretical binding model providing accurate values of binding constant (K_a), complex stoichiometry, and binding enthalpy (ΔH). The accuracy of the obtained values depends on how the data points are distributed along the sigmoidal isotherm. The form of the curve is related to the Wiseman value $c = n \times K_a \times [A]_{cell}$, where n is the number of binding sites per host, $[A]_{cell}$ is the concentration of the analyte (host or guest) in the reaction vessel (cell), and K_a is the average binding constant. Our experience suggests the use of c values between 10 and 500 is preferable to get a suitable curvature of the binding isotherm around the equivalence point. UV/Vis titrations allows one to determine association constants with limits at around 10^6–$10^7\ M^{-1}$. If the extinction coefficient of the compound is not large enough, one cannot acquire the corresponding absorption spectra. For example, working at 10^{-6} M requires an epsilon of $10^6\ M^{-1}\,cm^{-1}$ for having an absorbance of 1 (1 cm cuvette). When working in dilute conditions, if no changes are observed, most likely the binding constant is too small. However, the binding event is not always transduced in spectroscopic changes for a single technique. Fluorescence spectroscopy is more sensitive in terms of low concentrations. For instance, the highest binding constants of **11** and **12** for C_{60} were determined at host concentrations close to 10^{-9} M. Binding of squaraine dyes by **24** with $\log K = 8$ was investigated at 10^{-8} M concentration. Binding constants discussed in this review deliver the detection limit for fluorescence spectroscopy around $10^{10}\ M^{-1}$. In this vein, Thordarson highlighted in detail the key issues that need to be considered when planning supramolecular titration experiments and analyzing the obtained titration data.[125] He also provided online tools for determining accurate binding constants from titration experiments using local fitting and global analysis approaches.

6. Solvent Effects

Solvophobic interactions are maximized in water (hydrophobic effect). On the contrary, electrostatic interactions are stronger in nonpolar solvents and peak in the gas-phase. As shown by the Davis group, the recognition of carbohydrates in water (polar guests) is also driven by the hydrophobic effect. This was demonstrated by studying the binding properties of receptors **22a** and **22b** that are soluble in chloroform and in water, respectively. Accordingly, two derivatives of cellobiose were used owing to their solubilities either in chloroform or in water. The binding constant for receptor **22a** and cellobiose **G4** dropped from $3 \times 10^6\ M^{-1}$ to $11\ M^{-1}$ when the solvent was changed from a MeOH/$CHCl_3$ (0.5:99.5) mixture to pure MeOH. This result evidenced the competitive binding of the solvent for hydrogen bonding. Interestingly, CH_3CN, a polar nonprotic solvent, appeared to be even more disruptive for the host–guest formation next to DMSO and MeOH.[39] However, for the water-soluble host **22b**, the association constants for the cellobiose derivative grew as the amount of water in methanol was increased (Figure 12).

In contrast, ion–dipole interactions are maximized in organic solvents and decrease dramatically in water. Strong solvation of ions often disrupts electrostatic interactions. A representative example is the Kubik's macrocyclic peptide **64b** which can efficiently bind iodide and sulfate. However, its affinity drops three orders of magnitude when methanol is diluted with water.

If the binding is less effective, such as for flexible hosts with NH and CH-donors, then a linear affinity–solvent polarity relationship might be observed.[126] Such relationships can be used to determine the driving forces for the interactions in question. At least one example of a synthetic receptor that does not bind guests in $CHCl_3$ solution and becomes a good host in DMSO is known. Clearly, this is an exceptional case. The receptor featured an unfavorable conformation for binding in $CHCl_3$, the less polar solvent. This unproductive conformation was stabilized by intra-

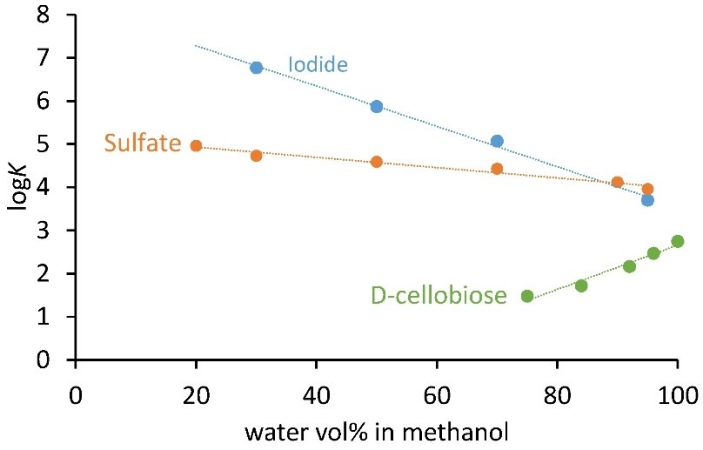

Figure 12. Dependence of the binding affinity (log*K*) on water content in the solvent mixture. The data were extracted from the anion binding studies of the Kubik's receptor **64b** with sulfate and iodide, and the Davis's receptor **22b** with cellobiose.

molecular hydrogen bonds that were disrupted in the polar and competitive DMSO.[127]

Overall, it is usually difficult to predict the effect of the solvent on the binding events because besides solvation, many other processes related to the host and guest structures are involved. The prediction of such effects at a qualitative level is still a current challenge.[128]

7. What Factors Contribute to Strong Host–Guest Binding?

A detailed analysis of the discussed host–guest synthetic systems allowed us to highlight several factors that influence strong binding. Often, it is a combination of several factors that leads to high binding affinity. For instance, solvation, preorganization, and functional complementarity of the binding sites are key in order to achieve strong binding. The 55 % filling factor (packing coefficient) of the closed cavity of the host by the encircled guest, a concept introduced by Collet[129] and Rebek,[130] is an important criterion to achieve strong binding in encapsulation complexes. Notably, for inclusion complexes, the calculation of the cavity volume is prone to significant variations. Nevertheless, as is common with any rule, there are exceptions. Talotta, Rescifina, Ballester, and Neri analyzed several geometric factors i.e., contact area, packing coefficient, and reorganization costs in the binding of alkylbenzylammonium guests by a calix[6]arene receptor in order to assess the best correlation with the stability of the induced-fit complexes.[131] The authors introduced a new parameter—expanding coefficient, which is determined as the ratio between the final (complex) and the initial (free host) cavity volumes displayed by the host in the corresponding energy-minimized structures. The binding constant values (log*K*) of the complexes of a calix[6]arene threaded with alkylbenzyl ammonim axles showed an excellent linear correlation with expanding coefficient, underlying the key impact of preorganization of the host geometry in binding affinity.

An interesting analysis of strong binding in enzyme–ligand interactions was carried out by Kuntz et al.[132] They discovered a sharp improvement in binding free energies in response to an increase in the number of heavy atoms in the structures of the ligands. At about 15 atoms, the binding free energy plateaus which corresponds to binding constants on the order of 10^{12} M^{-1}. According to the initial linear slope of the plot, the addition of one heavy atom in the ligand resulted in a gain of binding affinity of approximately -6.3 kJ mol^{-1} ($=1.5$ kcal mol^{-1}). Thus, a substantial binding affinity could be achieved with ligands containing only 7–10 heavy atoms. Most likely, this result is due to the dependency of the hydrophibic effect with the surface of the binding partners that is buried (removed from direct contact with water molecules) in the complex.

Also in water, the number of hydrogen bonds established between a host and a guest in the complex does not directly correlate with binding affinity. Other forces like the hydrophobic effect, van der Waals interactions, and factors not directly related to thermodynamics (e.g. structural features) might contribute to the binding dramatically. Some authors suggested that van der Waals interaction and the hydrophobic effect can contribute up to 1 kcal mol^{-1} (4.18 kJ mol^{-1}) per heavy atom when completely buried in the complex. Nevertheless, a minimum surface area is requested for this effect to be operative. As the number of atoms in the ligand increases, they shield each other, and their contribution decreases. Therefore, guest molecules with branched architectures may be the best choice to maximize surface/volume ratio. Receptor **24** for branched squaramide is a nice example of this type of interaction. The additional phenyl rings of the guest also increased the binding about 50-fold by establishing complementary π–π interactions in the outer sphere of the receptor.

In analogy to the binding sites of natural receptors, conformational rigidity and the three-dimensional arrangement of polar binding sites in the hydrophobic cavities of synthetic receptors are useful to shield the polar groups and the hydrophobic surfaces of the bound guests from solvent molecules. This strategy helps achieve high-affinity binding

even in water solution. In many cases, the formation of the complex leads to a severe reduction in the conformational flexibility of both host and guest molecules, which produces the observed enthalpy–entropy compensation effect. However, experimental data show that for concave synthetic cavities, which mainly bind guests through dispersion and hydrophobic interactions, the thermodynamic constants of the binding event deviate from those of the "nonclassical" hydrophobic effect. In this case, the thermodynamic signature expected for the "classical" hydrophobic effect is detected, that is a large and favorable entropic term due to the release of ordered solvating water molecules to the bulk and an enthalpy term close to zero. The involvement of the hydrophobic effect in a binding process is better evidenced by the large changes experienced in heat capacity with temperature rather than by its specific thermodynamic signature which may change significantly with temperature.

Another important effect playing a crucial role in strong binding is the presence of "high-energy" or better referred to as "high-enthalpy" water molecules. Hosts in which encapsulated water molecules are poorly stabilized by hydrogen bonding interactions display high-affinity binding for nonpolar substrates. For instance, the hydrophobic cavities of cucurbiturils do not involve electrostatic or polarizable interactions. However, the cucurbituril complexes of hydrophobic residues feature large stability constants in water. The binding process is enthalpically favored because "high-enthalpy" water molecules included in the host's cavity are released to the bulk solution and form additional hydrogen bonds.[133]

Analysis of strong interactions in Nature suggests that binding constants exceeding $10^{14}\,M^{-1}$ are rare and not always necessary. In the case of such high affinities, the binding kinetics (dissociation) could be too slow, and the solubility, production cost, and further functionalization of such ligands could be problematic. Thus, optimum affinities for the synthetic host to be used in biological settings should be in the range of the average values of $10^{8\pm2}\,M^{-1}$ observed in Nature. Nature uses multivalency to achieve very large binding affinities without compromising the reversibility (kinetic stability) of the formed aggregates.

7.1. Neutral Guests

Among the binding studies of aromatic guests in organic solvents, extraordinarily high association constants were achieved for fullerenes and their derivatives. Recognition of such guests benefits from the large surface area buried upon binding and the reduced/unsatisfactory solvation provided by the small molecules of nonpolar or polar solvents. Belt-shaped macrocyclic and tweezers-like receptors proved to be highly efficient in fullerene recognition. Crucial for recognition is the curved (concave) structure of the interacting π-systems to maximize van der Waals contacts. In some cases, extending the π-systems to make a wider belt did not have any effect on binding. However, the preorganization of the receptor's structure for the complex appeared to be beneficial to achieve strong binding. The superior solvation of the host–guest complexes of fullerenes compared to that of the binding partners is also key in achieving strong binding. A striking example of the solvophobic effect and electrostatic interactions in the binding of neutral polar guests is displayed by the palladium cage **33** that coordinates quinones in its polar cavity. While 1,4-cyclohexanone does not show any affinity for **33**, pentaquinone is bound with almost nanomolar affinity ($\log K = 8.9$) in CD_2Cl_2.[56] This example suggests that both electrostatic interactions and solvation effects turn-on in achieving the observed increase in binding affinity.

7.2. Positively Charged Guests

The design of receptors for positively charged guests often involves host structures having negatively charged carboxylic or sulfonic groups. This also explains the fact that many guests for this type of hosts are amines and polyamines, which become protonated in neutral or acidic water solutions. The binding strength of the resulting complex will be determined by the number of coulombic attractions that are present. Interestingly, there are cases in which the hydrophobic effect and dispersion interactions prevail over coulombic/electrostatic interactions. For instance, receptor **40** bearing two negative charges can coordinate the negatively charged NAD^+ in water solution. The arrangement of π-surfaces in shaping a hydrophobic cavity proved to be an efficient strategy to bind alkylammonium cations via a combination of cation–π and hydrophobic interactions. This strategy has allowed reaching even $10^9\,M^{-1}$ binding affinities for alkylammonium cations, e.g., in the case of naphthocages **47** and **48**.

7.3. Negatively Charged Guests

The ease of construction of receptors decorated with multiple alkylammonium groups allowed researchers to develop synthetic hosts for many anionic species. Macrocyclic polyammonium receptors represent a large group of anion-binding hosts. However, many of the receptors do not possess enough binding selectivity to be used in real applications due to the presence of competing anions. Coulombic interactions are not size- or shape-selective, and new designs are required to solve the selectivity problem.

Solvent effects can be as important as the strength of the noncovalent interactions. Sometimes solvents effects can be the major driving force for complexation.[134] As mentioned above, when the host binding sites were shielded from competitive hydrogen bonding solvents, for example, by using polar C–H hydrogen bond donors instead of $(NH)^+$ counterparts to coordinate anions, the sulfate anion was bound with a free binding energy of $\Delta G = -40\,kJ\,mol^{-1}$.[86]

In most cases, the association constants for anions dropped as the water content in the solution increased. This result derives from the stronger solvation of the polar binding sites by water molecules. However, there are several exceptions. For instance, receptor **64** is a dimeric receptor for sulfate consisting of two macrocyclic peptides as binding sites. **64** shows a minimal dependence of binding affinity on solvent

polarity owing to the strong hydrophobic interactions established between the two macrocycles that protected their polar binding groups and the bound sulfate and iodide ions from solvation with water molecules.

8. Summary and Outlook

In this review, we presented a collection of synthetic host–guest complexes with binding stabilities in the range of $10^6\ M^{-1}$ and higher. We classified the guests into three groups and showed major differences in the design approaches of their hosts. We revealed trends in binding affinity and selectivity for the discussed receptors. The relationships between the measured thermodynamic signatures of the binding events and the structural parameters of the interacting species were analyzed. We also summarized experimental results to emphasize several factors that might be helpful in the design of high-affinity receptors.

Nature offers a great variety of noncovalent interactions. Combining them results in the efficient recognition of small and large guests. Unfortunately, we cannot fully model all of them. Our knowledge to combine all of them in the design of the scaffolds of synthetic receptors in order to achieve high affinity and selectivity in binding is still limited. Guests possessing common structural features and functions, such as fullerenes, amines, and carboxylates, are bound with high affinities by synthetic receptors. On the contrary, the use of synthetic receptors for the strong and selective binding of guests bearing different functional groups and of those having reduced structural differences remains challenging. Strong intermolecular interactions open new perspectives to study supramolecular polymerization processes and design new materials with collective behaviors leading to new properties and hence unexpected applications. High-affinity receptors will also facilitate further investigations on how synthetic receptors interact with biological entities and help to discover new drugs.

Acknowledgements

E.A.K. thanks the Deutsche Forschungsgemeinschaft, projects KA 3444/16-1 and SFB 953. P.B. thanks Gobierno de España MICINN/AEI/FEDER (PID2020-114020GB-I00 and CEX2019-000925-S), the European Union (NOAH project H2020-MSCA-ITN project Ref. 765297), the CERCA Programme/Generalitat de Catalunya, and AGAUR (2017 SGR 1123) for current and continuous economic support. Open Access funding enabled and organized by Projekt DEAL.

Conflict of Interest

The authors declare no conflict of interest.

Keywords: Association Constants · Host–Guest Chemistry · Micromolar Affinity · Molecular Recognition · Noncovalent Interactions

[1] E. Fischer, *Ber. Dtsch. Chem. Ges.* **1894**, *27*, 2985–2993.
[2] H. P. Ferguson Johns, E. E. Harrison, K. J. Stingley, M. L. Waters, *Chem. Eur. J.* **2021**, *27*, 6620–6644.
[3] a) P. C. Weber, D. H. Ohlendorf, J. J. Wendoloski, F. R. Salemme, *Science* **1989**, *243*, 85–88; b) A. Chilkoti, P. S. Stayton, *J. Am. Chem. Soc.* **1995**, *117*, 10622–10628.
[4] J. DeChancie, K. N. Houk, *J. Am. Chem. Soc.* **2007**, *129*, 5419–5429.
[5] H. K. Nair, K. Lee, D. M. Quinn, *J. Am. Chem. Soc.* **1993**, *115*, 9939–9941.
[6] M. C. Rose, R. W. Henkens, *Biochim. Biophys. Acta Gen. Subj.* **1974**, *372*, 426–435.
[7] L. Dupont, I. Garcia, M. C. Poggi, G. Alloing, K. Mandon, D. Le Rudulier, *J. Bacteriol.* **2004**, *186*, 5988–5996.
[8] L. M. Salonen, M. Ellermann, F. Diederich, *Angew. Chem. Int. Ed.* **2011**, *50*, 4808–4842; *Angew. Chem.* **2011**, *123*, 4908–4944.
[9] a) V. G. H. Lafitte, A. E. Aliev, P. N. Horton, M. B. Hursthouse, K. Bala, P. Golding, H. C. Hailes, *J. Am. Chem. Soc.* **2006**, *128*, 6544–6545; b) H. Q. Zeng, R. S. Miller, R. A. Flowers, B. Gong, *J. Am. Chem. Soc.* **2000**, *122*, 2635–2644.
[10] W. L. Jorgensen, J. Pranata, *J. Am. Chem. Soc.* **1990**, *112*, 2008–2010.
[11] P. Motloch, C. A. Hunter in *Advances in Physical Organic Chemistry, Vol. 50* (Eds.: I. H. Williams, N. H. Williams), Academic Press, New York, **2016**, pp. 77–118.
[12] H.-J. Schneider, *Angew. Chem. Int. Ed. Engl.* **1991**, *30*, 1417–1436; *Angew. Chem.* **1991**, *103*, 1419–1439.
[13] a) S. J. Barrow, S. Kasera, M. J. Rowland, J. del Barrio, O. A. Scherman, *Chem. Rev.* **2015**, *115*, 12320–12406; b) H. Nie, Z. Wei, X.-L. Ni, Y. Liu, *Chem. Rev.* **2022**, *122*, 9032–9077; c) K. I. Assaf, W. M. Nau, *Chem. Soc. Rev.* **2015**, *44*, 394–418.
[14] R. N. Dsouza, U. Pischel, W. M. Nau, *Chem. Rev.* **2011**, *111*, 7941–7980.
[15] L. Isaacs, *Acc. Chem. Res.* **2014**, *47*, 2052–2062.
[16] D. Das, K. I. Assaf, W. M. Nau, *Front. Chem.* **2019**, *7*, 619.
[17] a) L. Zoppi, J. S. Siegel, K. K. Baldridge, *Wiley Interdiscip. Rev. Comput. Mol. Sci.* **2013**, *3*, 1–12; b) Y. Xu, M. von Delius, *Angew. Chem. Int. Ed.* **2020**, *59*, 559–573; *Angew. Chem.* **2020**, *132*, 567–582.
[18] S. Goodarzi, T. Da Ros, J. Conde, F. Sefat, M. Mozafari, *Mater. Today* **2017**, *20*, 460–480.
[19] E. Castro, A. H. Garcia, G. Zavala, L. Echegoyen, *J. Mater. Chem. B* **2017**, *5*, 6523–6535.
[20] M. Park, K. I. Hong, M. Kang, T. W. Kim, H. Lee, W. D. Jang, K. U. Jeong, *ACS Nano* **2019**, *13*, 6101–6112.
[21] G. Gil-Ramírez, S. D. Karlen, A. Shundo, K. Porfyrakis, Y. Ito, G. A. D. Briggs, J. J. L. Morton, H. L. Anderson, *Org. Lett.* **2010**, *12*, 3544–3547.
[22] F. Hajjaj, K. Tashiro, H. Nikawa, N. Mizorogi, T. Akasaka, S. Nagase, K. Furukawa, T. Kato, T. Aida, *J. Am. Chem. Soc.* **2011**, *133*, 9290–9292.
[23] C. García-Simón, M. Garcia-Borràs, L. Gómez, T. Parella, S. Osuna, J. Juanhuix, I. Imaz, D. Maspoch, M. Costas, X. Ribas, *Nat. Commun.* **2014**, *5*, 5557.
[24] C. Fuertes-Espinosa, C. Garcia-Simon, M. Pujals, M. Garcia-Borras, L. Gomez, T. Parella, J. Juanhuix, I. Imaz, D. Maspoch, M. Costas, X. Ribas, *Chem* **2020**, *6*, 169–186.
[25] M. Yanagisawa, K. Tashiro, M. Yamasaki, T. Aida, *J. Am. Chem. Soc.* **2007**, *129*, 11912–11913.

[26] Y. Xu, S. Gsänger, M. B. Minameyer, I. Imaz, D. Maspoch, O. Shyshov, F. Schwer, X. Ribas, T. Drewello, B. Meyer, M. von Delius, *J. Am. Chem. Soc.* **2019**, *141*, 18500–18507.

[27] a) F. Schwer, S. Zank, M. Freiberger, R. Kaur, S. Frühwald, C. C. Robertson, A. Görling, T. Drewello, D. M. Guldi, M. von Delius, *Org. Mater.* **2022**, *4*, 7–17; b) T. Iwamoto, Y. Watanabe, T. Sadahiro, T. Haino, S. Yamago, *Angew. Chem. Int. Ed.* **2011**, *50*, 8342–8344; *Angew. Chem.* **2011**, *123*, 8492–8494.

[28] H. Isla, M. Gallego, E. M. Pérez, R. Viruela, E. Ortí, N. Martín, *J. Am. Chem. Soc.* **2010**, *132*, 1772–1773.

[29] S. Hitosugi, R. Iizuka, T. Yamasaki, R. Zhang, Y. Murata, H. Isobe, *Org. Lett.* **2013**, *15*, 3199–3201.

[30] H. Isobe, S. Hitosugi, T. Yamasaki, R. Iizuka, *Chem. Sci.* **2013**, *4*, 1293–1297.

[31] T. Matsuno, S. Kamata, S. Sato, A. Yokoyama, P. Sarkar, H. Isobe, *Angew. Chem. Int. Ed.* **2017**, *56*, 15020–15024; *Angew. Chem.* **2017**, *129*, 15216–15220.

[32] Q. Huang, G. Zhuang, H. Jia, M. Qian, S. Cui, S. Yang, P. Du, *Angew. Chem. Int. Ed.* **2019**, *58*, 6244–6249; *Angew. Chem.* **2019**, *131*, 6310–6315.

[33] D. Lu, G. Zhuang, H. Wu, S. Wang, S. Yang, P. Du, *Angew. Chem. Int. Ed.* **2017**, *56*, 158–162; *Angew. Chem.* **2017**, *129*, 164–168.

[34] M. Takeda, S. Hiroto, H. Yokoi, S. Lee, D. Kim, H. Shinokubo, *J. Am. Chem. Soc.* **2018**, *140*, 6336–6342.

[35] F. Diederich, K. Dick, *J. Am. Chem. Soc.* **1984**, *106*, 8024–8036.

[36] D. B. Smithrud, F. Diederich, *J. Am. Chem. Soc.* **1990**, *112*, 339–343.

[37] M. Bria, G. Cooke, A. Cooper, J. F. Garety, S. G. Hewage, M. Nutley, G. Rabani, P. Woisel, *Tetrahedron Lett.* **2007**, *48*, 301–304.

[38] Y. Ohishi, K. Masuda, K. Kudo, H. Abe, M. Inouye, *Chem. Eur. J.* **2021**, *27*, 785–793.

[39] E. Klein, Y. Ferrand, N. P. Barwell, A. P. Davis, *Angew. Chem. Int. Ed.* **2008**, *47*, 2693–2696; *Angew. Chem.* **2008**, *120*, 2733–2736.

[40] S. K. Chang, A. D. Hamilton, *J. Am. Chem. Soc.* **1988**, *110*, 1318–1319.

[41] M. Ali, E. Kataev, J. Muller, H. Park, M. Halik, A. Hirsch, *Chem. Eur. J.* **2021**, *27*, 16429–16439.

[42] J. J. Gassensmith, E. Arunkumar, L. Barr, J. M. Baumes, K. M. DiVittorio, J. R. Johnson, B. C. Noll, B. D. Smith, *J. Am. Chem. Soc.* **2007**, *129*, 15054–15059.

[43] E. M. Peck, W. Q. Liu, G. T. Spence, S. K. Shaw, A. P. Davis, H. Destecroix, B. D. Smith, *J. Am. Chem. Soc.* **2015**, *137*, 8668–8671.

[44] M. Dharmarwardana, J. M. Dempsey, S. Padilla-Coley, T. S. Jarvis, K. Shi, K. M. Atkinson, B. D. Smith, *Chem. Commun.* **2021**, *57*, 13518–13521.

[45] W. Liu, A. Johnson, B. D. Smith, *J. Am. Chem. Soc.* **2018**, *140*, 3361–3370.

[46] H. Yao, H. Ke, X. Zhang, S.-J. Pan, M.-S. Li, L.-P. Yang, G. Schreckenbach, W. Jiang, *J. Am. Chem. Soc.* **2018**, *140*, 13466–13477.

[47] Z. Chen, M. Quan, Y. W. Dong, M. S. Li, S. M. Wang, L. M. Zhao, L. P. Yang, J. S. Wu, W. Jiang, *Chem. Commun.* **2022**, *58*, 9413–9416.

[48] H. Zhang, L.-L. Wang, X.-Y. Pang, L.-P. Yang, W. Jiang, *Chem. Commun.* **2021**, *57*, 13724–13727.

[49] H. Zhou, X.-Y. Pang, X. Wang, H. Yao, L.-P. Yang, W. Jiang, *Angew. Chem. Int. Ed.* **2021**, *60*, 25981–25987; *Angew. Chem.* **2021**, *133*, 26185–26191.

[50] N. Kishida, K. Matsumoto, Y. Tanaka, M. Akita, H. Sakurai, M. Yoshizawa, *J. Am. Chem. Soc.* **2020**, *142*, 9599–9603.

[51] W. Liu, S. Bobbala, C. L. Stern, J. E. Hornick, Y. Liu, A. E. Enciso, E. A. Scott, J. F. Stoddart, *J. Am. Chem. Soc.* **2020**, *142*, 3165–3173.

[52] K. Ono, J. K. Klosterman, M. Yoshizawa, K. Sekiguchi, T. Tahara, M. Fujita, *J. Am. Chem. Soc.* **2009**, *131*, 12526–12527.

[53] S. Tashiro, M. Kobayashi, M. Fujita, *J. Am. Chem. Soc.* **2006**, *128*, 9280–9281.

[54] S. Turega, W. Cullen, M. Whitehead, C. A. Hunter, M. D. Ward, *J. Am. Chem. Soc.* **2014**, *136*, 8475–8483.

[55] W. Cullen, S. Turega, C. A. Hunter, M. D. Ward, *Chem. Sci.* **2015**, *6*, 2790–2794.

[56] D. P. August, G. S. Nichol, P. J. Lusby, *Angew. Chem. Int. Ed.* **2016**, *55*, 15022–15026; *Angew. Chem.* **2016**, *128*, 15246–15250.

[57] T. Guinovart, D. Hernandez-Alonso, L. Adriaenssens, P. Blondeau, M. Martinez-Belmonte, F. X. Rius, F. J. Andrade, P. Ballester, *Angew. Chem. Int. Ed.* **2016**, *55*, 2435–2440; *Angew. Chem.* **2016**, *128*, 2481–2486.

[58] L. Escobar, G. Aragay, P. Ballester, *Chem. Eur. J.* **2016**, *22*, 13682–13689.

[59] L. Escobar, P. Ballester, *Org. Chem. Front.* **2019**, *6*, 1738–1748.

[60] G. Peñuelas-Haro, P. Ballester, *Chem. Sci.* **2019**, *10*, 2413–2423.

[61] A. Galán, E. C. Escudero-Adán, A. Frontera, P. Ballester, *J. Org. Chem.* **2014**, *79*, 5545–5557.

[62] L. Escobar, F. A. Arroyave, P. Ballester, *Eur. J. Org. Chem.* **2018**, 1097–1106.

[63] G. Moncelsi, L. Escobar, H. Dube, P. Ballester, *Chem. Asian J.* **2018**, *13*, 1632–1639.

[64] L. Chen, H.-Y. Zhang, Y. Liu, *J. Org. Chem.* **2012**, *77*, 9766–9773.

[65] G. Yu, X. Zhou, Z. Zhang, C. Han, Z. Mao, C. Gao, F. Huang, *J. Am. Chem. Soc.* **2012**, *134*, 19489–19497.

[66] D. Xia, P. Wang, B. Shi, *Org. Biomol. Chem.* **2017**, *15*, 7618–7622.

[67] G. Ghale, A. G. Lanctot, H. T. Kreissl, M. H. Jacob, H. Weingart, M. Winterhalter, W. M. Nau, *Angew. Chem. Int. Ed.* **2014**, *53*, 2762–2765; *Angew. Chem.* **2014**, *126*, 2801–2805.

[68] L. Vial, R. F. Ludlow, J. Leclaire, R. Pérez-Fernández, S. Otto, *J. Am. Chem. Soc.* **2006**, *128*, 10253–10257.

[69] M. Heilmann, M. Knezevic, G. Piccini, K. Tiefenbacher, *Org. Biomol. Chem.* **2021**, *19*, 3628–3633.

[70] X. N. Han, P. F. Li, Y. Han, C. F. Chen, *Angew. Chem. Int. Ed.* **2022**, *61*, e202202527; *Angew. Chem.* **2022**, *134*, e202202527.

[71] S.-B. Lu, H. Chai, J. S. Ward, M. Quan, J. Zhang, K. Rissanen, R. Luo, L.-P. Yang, W. Jiang, *Chem. Commun.* **2020**, *56*, 888–891.

[72] C. Jia, W. Zuo, D. Yang, Y. Chen, L. Cao, R. Custelcean, J. Hostaš, P. Hobza, R. Glaser, Y.-Y. Wang, X.-J. Yang, B. Wu, *Nat. Commun.* **2017**, *8*, 938.

[73] S. V. Rosokha, J. K. Kochi, *J. Am. Chem. Soc.* **2002**, *124*, 5620–5621.

[74] a) K. D. Daze, T. Pinter, C. S. Beshara, A. Ibraheem, S. A. Minaker, M. C. F. Ma, R. J. M. Courtemanche, R. E. Campbell, F. Hof, *Chem. Sci.* **2012**, *3*, 2695–2699; b) S. Tabet, S. F. Douglas, K. D. Daze, G. A. E. Garnett, K. J. H. Allen, E. M. M. Abrioux, T. T. H. Quon, J. E. Wulff, F. Hof, *Bioorg. Med. Chem.* **2013**, *21*, 7004–7010.

[75] N. K. Pinkin, M. L. Waters, *Org. Biomol. Chem.* **2014**, *12*, 7059–7067.

[76] I. N. Gober, M. L. Waters, *Org. Biomol. Chem.* **2017**, *15*, 7789–7795.

[77] V. McKee, J. Nelson, R. M. Town, *Chem. Soc. Rev.* **2003**, *32*, 309–325.

[78] C. A. Ilioudis, D. A. Tocher, J. W. Steed, *J. Am. Chem. Soc.* **2004**, *126*, 12395–12402.

[79] B. Dietrich, B. Dilworth, J. M. Lehn, J. P. Souchez, M. Cesario, J. Guilhem, C. Pascard, *Helv. Chim. Acta* **1996**, *79*, 569–587.

[80] R. R. Mittapalli, S. S. R. Namashivaya, A. S. Oshchepkov, E. Kuczynska, E. A. Kataev, *Chem. Commun.* **2017**, *53*, 4822–4825.

[81] H. Ihm, S. Yun, H. G. Kim, J. K. Kim, K. S. Kim, *Org. Lett.* **2002**, *4*, 2897–2900.

[82] a) Y. Hu, S. Long, H. Fu, Y. She, Z. Xu, J. Yoon, *Chem. Soc. Rev.* **2021**, *50*, 589–618; b) J. Yoon, S. K. Kim, N. J. Singh, K. S. Kim, *Chem. Soc. Rev.* **2006**, *35*, 355–360.

[83] Z. C. Xu, J. Y. Choi, J. Yoon, *Bull. Korean Chem. Soc.* **2011**, *32*, 1371–1374.

[84] a) D. Zhang, X. Jiang, Z. Dong, H. Yang, A. Martinez, G. Gao, *Tetrahedron* **2013**, *69*, 10457–10462; b) D. P. Cormode, S. S. Murray, A. R. Cowley, P. D. Beer, *Dalton Trans.* **2006**, 5135–5140.

[85] N. Ahmed, B. Shirinfar, I. S. Youn, A. Bist, V. Suresh, K. S. Kim, *Chem. Commun.* **2012**, *48*, 2662–2664.

[86] J. Cai, B. P. Hay, N. J. Young, X. Yang, J. L. Sessler, *Chem. Sci.* **2013**, *4*, 1560–1567.

[87] P. Sokkalingam, D. S. Kim, H. Hwang, J. L. Sessler, C.-H. Lee, *Chem. Sci.* **2012**, *3*, 1819.

[88] V. Amendola, M. Boiocchi, L. Fabbrizzi, N. Fusco, *Eur. J. Org. Chem.* **2011**, 6434–6444.

[89] D. Grell, E. Grell, P. Bugnon, B. Dietrich, J. M. Lehn, *J. Therm. Anal. Calorim.* **2004**, *77*, 483–495.

[90] Z. Rodriguez-Docampo, E. Eugenieva-Ilieva, C. Reyheller, A. M. Belenguer, S. Kubik, S. Otto, *Chem. Commun.* **2011**, *47*, 9798–9800.

[91] Z. Rodriguez-Docampo, S. I. Pascu, S. Kubik, S. Otto, *J. Am. Chem. Soc.* **2006**, *128*, 11206–11210.

[92] F. Sommer, S. Kubik, *Org. Biomol. Chem.* **2014**, *12*, 8851–8860.

[93] R. Ning, Y.-F. Ao, D.-X. Wang, Q.-Q. Wang, *Chem. Eur. J.* **2018**, *24*, 4268–4272.

[94] J. H. Oh, J. H. Kim, D. S. Kim, H. J. Han, V. M. Lynch, J. L. Sessler, S. K. Kim, *Org. Lett.* **2019**, *21*, 4336–4339.

[95] H. J. Han, J. H. Oh, J. L. Sessler, S. K. Kim, *Chem. Commun.* **2019**, *55*, 10876–10879.

[96] E. A. Katayev, J. L. Sessler, V. N. Khrustalev, Y. A. Ustynyuk, *J. Org. Chem.* **2007**, *72*, 7244–7252.

[97] K. I. Assaf, B. Begaj, A. Frank, M. Nilam, A. S. Mougharbel, U. Kortz, J. Nekvinda, B. Grüner, D. Gabel, W. M. Nau, *J. Org. Chem.* **2019**, *84*, 11790–11798.

[98] K. I. Assaf, J. Holub, E. Bernhardt, J. M. Oliva-Enrich, M. I. Fernández Pérez, M. Canle, J. A. Santaballa, J. Fanfrlík, D. Hnyk, W. M. Nau, *ChemPhysChem* **2020**, *21*, 971–976.

[99] K. Fujita, S. Ejima, T. Imoto, *J. Chem. Soc. Chem. Commun.* **1984**, 1277–1278.

[100] R. C. Petter, C. T. Sikorski, D. H. Waldeck, *J. Am. Chem. Soc.* **1991**, *113*, 2325–2327.

[101] Z. Zheng, H. Yu, W.-C. Geng, X.-Y. Hu, Y.-Y. Wang, Z. Li, Y. Wang, D.-S. Guo, *Nat. Commun.* **2019**, *10*, 5762.

[102] Z. Zheng, W.-C. Geng, J. Gao, Y.-Y. Wang, H. Sun, D.-S. Guo, *Chem. Sci.* **2018**, *9*, 2087–2091.

[103] a) Y.-Y. Wang, Y. Kong, Z. Zheng, W.-C. Geng, Z.-Y. Zhao, H. Sun, D.-S. Guo, *Beilstein J. Org. Chem.* **2019**, *15*, 1394–1406; b) S.-Y. Yao, Y.-X. Yue, A.-K. Ying, X.-Y. Hu, H.-B. Li, K. Cai, D.-S. Guo, *Angew. Chem. Int. Ed.* **2023**, *62*, e202213578; *Angew. Chem.* **2023**, *135*, e202213578. c) S. Li, R. Ma, X.-Y. Hu, H.-B. Li, W.-C. Geng, X. Kong, C. Zhang, D.-S. Guo, *Adv. Mater.* **2022**, *34*, 2203765.

[104] Z. Zawada, A. Tatar, P. Mocilac, M. Budesinsky, T. Kraus, *Angew. Chem. Int. Ed.* **2018**, *57*, 9891–9895; *Angew. Chem.* **2018**, *130*, 10039–10043.

[105] B. Dietrich, M. W. Hosseini, J. M. Lehn, R. B. Sessions, *J. Am. Chem. Soc.* **1981**, *103*, 1282–1283.

[106] E. Kimura, M. Kodama, T. Yatsunami, *J. Am. Chem. Soc.* **1982**, *104*, 3182–3187.

[107] H. Fenniri, M. W. Hosseini, J. M. Lehn, *Helv. Chim. Acta* **1997**, *80*, 786–803.

[108] P. Čudić, M. Žinić, V. Tomišić, V. Simeon, J. P. Vigneron, J. M. Lehn, *J. Chem. Soc. Chem. Commun.* **1995**, 1073–1075.

[109] a) M. Inouye, K. Fujimoto, M. Furusyo, H. Nakazumi, *J. Am. Chem. Soc.* **1999**, *121*, 1452–1458; b) H. Abe, Y. Mawatari, H. Teraoka, K. Fujimoto, M. Inouye, *J. Org. Chem.* **2004**, *69*, 495–504.

[110] J. L. Sessler, D. Q. An, W. S. Cho, V. Lynch, M. Marquez, *Chem. Commun.* **2005**, 540–542.

[111] a) J.-F. Ayme, J. E. Beves, C. J. Campbell, G. Gil-Ramírez, D. A. Leigh, A. J. Stephens, *J. Am. Chem. Soc.* **2015**, *137*, 9812–9815; b) L. Zhang, A. J. Stephens, J. F. Lemonnier, L. Pirvu, I. J. Vitorica-Yrezabal, C. J. Robinson, D. A. Leigh, *J. Am. Chem. Soc.* **2019**, *141*, 3952–3958.

[112] S.-D. Jeong, J. Yoo, H.-K. Na, D. Y. Chi, C.-H. Lee, *Supramol. Chem.* **2007**, *19*, 271–275.

[113] D. W. Yoon, D. E. Gross, V. M. Lynch, J. L. Sessler, B. P. Hay, C. H. Lee, *Angew. Chem. Int. Ed.* **2008**, *47*, 5038–5042; *Angew. Chem.* **2008**, *120*, 5116–5120.

[114] W. Chen, C. Guo, Q. He, X. Chi, V. M. Lynch, Z. Zhang, J. Su, H. Tian, J. L. Sessler, *J. Am. Chem. Soc.* **2019**, *141*, 14798–14806.

[115] S. J. Edwards, H. Valkenier, N. Busschaert, P. A. Gale, A. P. Davis, *Angew. Chem. Int. Ed.* **2015**, *54*, 4592–4596; *Angew. Chem.* **2015**, *127*, 4675–4679.

[116] a) K. P. McDonald, Y. R. Hua, S. Lee, A. H. Flood, *Chem. Commun.* **2012**, *48*, 5065–5075; b) E. M. Zahran, Y. Hua, Y. Li, A. H. Flood, L. G. Bachas, *Anal. Chem.* **2010**, *82*, 368–375.

[117] Y. Liu, A. Sengupta, K. Raghavachari, A. H. Flood, *Chem* **2017**, *3*, 411–427.

[118] Y. Liu, W. Zhao, C. H. Chen, A. H. Flood, *Science* **2019**, *365*, 159–161.

[119] J. Mosquera, S. Zarra, J. R. Nitschke, *Angew. Chem. Int. Ed.* **2014**, *53*, 1556–1559; *Angew. Chem.* **2014**, *126*, 1582–1585.

[120] K. Niki, T. Tsutsui, M. Yamashina, M. Akita, M. Yoshizawa, *Angew. Chem. Int. Ed.* **2020**, *59*, 10489–10492; *Angew. Chem.* **2020**, *132*, 10575–10578.

[121] V. Havel, J. Svec, M. Wimmerova, M. Dusek, M. Pojarova, V. Sindelar, *Org. Lett.* **2011**, *13*, 4000–4003.

[122] M. A. Yawer, V. Havel, V. Sindelar, *Angew. Chem. Int. Ed.* **2015**, *54*, 276–279; *Angew. Chem.* **2015**, *127*, 278–281.

[123] M. R. Sullivan, P. Sokkalingam, T. Nguyen, J. P. Donahue, B. C. Gibb, *J. Comput.-Aided Mol. Des.* **2017**, *31*, 21–28.

[124] P. Suating, T. T. Nguyen, N. E. Ernst, Y. Wang, J. H. Jordan, C. L. D. Gibb, H. S. Ashbaugh, B. C. Gibb, *Chem. Sci.* **2020**, *11*, 3656–3663.

[125] P. Thordarson, *Chem. Soc. Rev.* **2011**, *40*, 1305–1323.

[126] T. J. Sherbow, H. A. Fargher, M. M. Haley, M. D. Pluth, D. W. Johnson, *J. Org. Chem.* **2020**, *85*, 12367–12373.

[127] S. Rossi, G. M. Kyne, D. L. Turner, N. J. Wells, J. D. Kilburn, *Angew. Chem. Int. Ed.* **2002**, *41*, 4233–4236; *Angew. Chem.* **2002**, *114*, 4407–4409.

[128] M. D. Driver, M. J. Williamson, J. L. Cook, C. A. Hunter, *Chem. Sci.* **2020**, *11*, 4456–4466.

[129] L. Garel, J. P. Dutasta, A. Collet, *Angew. Chem. Int. Ed. Engl.* **1993**, *32*, 1169–1171; *Angew. Chem.* **1993**, *105*, 1249–1251.

[130] S. Mecozzi, J. Rebek, *Chem. Eur. J.* **1998**, *4*, 1016–1022.

[131] C. Talotta, G. Concilio, M. De Rosa, A. Soriente, C. Gaeta, A. Rescifina, P. Ballester, P. Neri, *Org. Lett.* **2021**, *23*, 1804–1808.
[132] I. D. Kuntz, K. Chen, K. A. Sharp, P. A. Kollman, *Proc. Natl. Acad. Sci. USA* **1999**, *96*, 9997–10002.
[133] F. Biedermann, W. M. Nau, H.-J. Schneider, *Angew. Chem. Int. Ed.* **2014**, *53*, 11158–11171; *Angew. Chem.* **2014**, *126*, 11338–11352.
[134] F. Würthner, *J. Org. Chem.* **2022**, *87*, 1602–1615.

Manuscript received: October 6, 2022
Accepted manuscript online: November 23, 2022
Version of record online: ■■, ■■

Reviews

Host-Guest Complexes

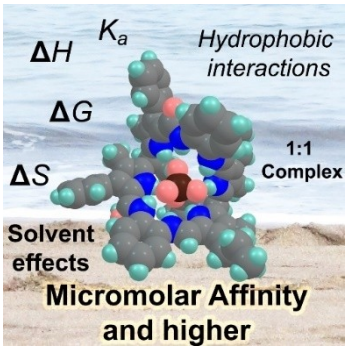

The review collects recent achievements in the design of 1:1 host–guest complexes with association constants exceeding 10^6 M^{-1}. The relationships between the measured thermodynamic constants and the structural parameters of the interacting species are analyzed. The design features of high-affinity hosts are discussed in light of their binding properties. Hints are provided for the design of future receptors displaying high affinity and selectivity.